

FINAL REPORT

Nanofiber-Enabled, Multi-Target Passive Sampling Device for
Determination of the Freely-Dissolved Sediment Pore Water
Concentrations of Organic Contaminants

SERDP Project ER-2543

JUNE 2016

Dr. Andres Martinez
Dr. David M. Cwiertny
The University of Iowa

Distribution Statement A

This document has been cleared for public release



Page Intentionally Left Blank

This report was prepared under contract to the Department of Defense Strategic Environmental Research and Development Program (SERDP). The publication of this report does not indicate endorsement by the Department of Defense, nor should the contents be construed as reflecting the official policy or position of the Department of Defense. Reference herein to any specific commercial product, process, or service by trade name, trademark, manufacturer, or otherwise, does not necessarily constitute or imply its endorsement, recommendation, or favoring by the Department of Defense.

Page Intentionally Left Blank

REPORT DOCUMENTATION PAGE

Form Approved
OMB No. 0704-0188

Public reporting burden for this collection of information is estimated to average 1 hour per response, including the time for reviewing instructions, searching existing data sources, gathering and maintaining the data needed, and completing and reviewing this collection of information. Send comments regarding this burden estimate or any other aspect of this collection of information, including suggestions for reducing this burden to Department of Defense, Washington Headquarters Services, Directorate for Information Operations and Reports (0704-0188), 1215 Jefferson Davis Highway, Suite 1204, Arlington, VA 22202-4302. Respondents should be aware that notwithstanding any other provision of law, no person shall be subject to any penalty for failing to comply with a collection of information if it does not display a currently valid OMB control number. **PLEASE DO NOT RETURN YOUR FORM TO THE ABOVE ADDRESS.**

1. REPORT DATE (DD-MM-YYYY) 06-01-2016		2. REPORT TYPE Final report		3. DATES COVERED (From - To) May 2015 June 2016	
4. TITLE AND SUBTITLE NANOFIBER-ENABLED, MULTI-TARGET PASSIVE SAMPLING DEVICE FOR DETERMINATION OF THE FREELY-DISSOLVED SEDIMENT PORE WATER				5a. CONTRACT NUMBER W912HQ-15-P-0022	
				5b. GRANT NUMBER ER-2543	
				5c. PROGRAM ELEMENT NUMBER	
6. AUTHOR(S) Martinez, Andres Cwiertny, David M.				5d. PROJECT NUMBER	
				5e. TASK NUMBER	
				5f. WORK UNIT NUMBER	
7. PERFORMING ORGANIZATION NAME(S) AND ADDRESS(ES) The University of Iowa 105 Jessup Hall, Iowa City, IA 52242-1316				8. PERFORMING ORGANIZATION REPORT NUMBER	
9. SPONSORING / MONITORING AGENCY NAME(S) AND ADDRESS(ES) SERDP/ESTCP Program Office 4800 Mark Center Drive, Suite Alexandria, VA 22350-3600				10. SPONSOR/MONITOR'S ACRONYM(S) SERDP/ESTCP	
				11. SPONSOR/MONITOR'S REPORT NUMBER(S)	
12. DISTRIBUTION / AVAILABILITY STATEMENT unlimited					
13. SUPPLEMENTARY NOTES					
14. ABSTRACT We used electrospinning to fabricate a suite of electrospun nanofiber mats (ENMs) and test their sorption capacities to a set of hydrophilic (aniline and nitrobenzene) and hydrophobic compounds (PCBs and Dioxin) to be used as next-generation multi-target passive samplers. The average diameter of the ENMs ranged from 70 (PET) to 1,000 (EVA) nm, with a relative standard deviation of less than 50% for each material. Our ENMs in water yielded a fast equilibration time (< 3 days) for our tested hydrophilic and hydrophobic compounds. The ENM-water partition coefficient (K_{ENM-w}) for the hydrophilic compounds ranged from 0.72 to 2.8 log units, with evidence suggesting uptake via partitioning into the bulk nanofiber (i.e. absorption) and specific binding interactions (e.g., H-bonding and Coulombic interactions) contributing to, and potentially controlling, hydrophilic uptake. The K_{ENM-w} for hydrophobic compounds ranged from 3.2 to 6.4 log units. Collectively, the rates and K_{ENM-w} measured for the best performing ENMs often exceeded partition coefficients achieved with commercially available passive sampling materials (e.g., low-density polyethylene and PDMS glass fiber), particularly for hydrophilic compounds. Overall, our results support our initial hypothesis that electrospun nanofiber mats represent next-generation passive sampling materials that can be easily modified to enhance compound selectivity, sorption capacities and improve field applications.					
15. SUBJECT TERMS Electrospinning, hydrophilic and hydrophobic compounds, munitions constituents, sediment pore water, passive sampling materials.					
16. SECURITY CLASSIFICATION OF:			17. LIMITATION OF ABSTRACT UU	18. NUMBER OF PAGES 58	19a. NAME OF RESPONSIBLE PERSON Andres Martinez
a. REPORT U	b. ABSTRACT U	c. THIS PAGE U			19b. TELEPHONE NUMBER (include area code) 319-471-3070

Page Intentionally Left Blank

Table of Contents

List of Tables	iii
List of Figures	iii
List of Acronyms	vii
Keywords	vii
Acknowledgements.....	vii
Abstract	1
Objective	3
Background.....	5
Opportunities in passive sampler development.....	5
Electrospun nanofiber mats as a next-generation passive sampling platform	6
Material and Methods	8
Synthesis of Electrospun Polymer Nanofiber Mats (ENMs)	8
Preparation of Chemically Modified ENMs and ENM Composites.....	11
Preparation of Multilayer ENMs.....	12
ENMs Characterization, Stability and Strength Testing	12
Target analytes	13
Uptake and ENM-Water Equilibrium Partition Coefficient Experiments	14
Soil Preparation and Uptake Experiments	15
Contaminated Sediment Measurements	16
Analytical Methods	16
Aniline and Nitrobenzene	17
PCBs and Dioxin.....	17
Quality Assurance and Control (QA/QC)	17
Aniline and Nitrobenzene	17
PCBs and Dioxin.....	18
Results and Discussions.....	18
Synthesis of ENMs via Electrospinning.....	18
Characterization of ENMs Nanofiber Surface Area, Diameter and Thickness.....	20
Mechanical Testing and Chemical Stability of ENMs.....	22
Chemical Modification of ENMs and ENM Composites	23
Fabrication of Multilayer ENMs	24
Determination of Uptake Kinetics and ENM-Water Equilibrium Partition Coefficients	24
Polar Analytes: Aniline and Nitrobenzene	24
Hydrophobic Analytes: PCBs and Dioxin	26
Influence of solution phase variables on performance of most promising ENMs.....	28
Influence of pH on aniline and nitrobenzene uptake	28

Influence of Aniline and Nitrobenzene concentration on ENM-Water Partitioning	29
ENM Performance in Multi-Target Pollutant Mixtures.....	30
Further Optimization of Promising ENMs to Improve Sampler Performance	30
Influence of ENM average diameter on polar analyte uptake	30
Influence of CNT integration on polar analyte uptake.	30
Influence of CNT integration on hydrophobic analyte uptake.	32
Influence of cationic and anionic surfactant integration on polar analyte uptake.	32
Influence of chemical functionalization via amidoximation on polar analyte uptake.	33
Influence of biocidal agents on polar analyte uptake.....	33
Performance of multilayer ENMs.	34
Summary of all ENM performance tests and comparison to commercially available materials.	35
Freely-Dissolved Pore Water Measurements	38
Spiked Model Soil Systems	38
Contaminated Sediment Systems.....	41
Conclusions and Implications for Future Research	42
Key Results	42
Tangible outcomes and products	42
Overarching implications of SEED project results and outcomes.....	43
Opportunities for future research	43
Literature Cited	46

List of Tables

Table 1. Reagents, physical and chemical properties, and electrospinning synthesis parameters for ENMs investigated herein.	10
Table 2. Name and select physicochemical properties of the analytes (i.e., pollutant targets) investigated herein. Sources of data are listed in parenthesis.	13
Table 3. Summary of the analytes and polymers for which ENM-water equilibrium partition coefficients were measured experimentally in homogeneous (water) systems.	15
Table 4. Summary table of the ENMs and analytes used in the spiked model soil experiments performed.	16
Table 5. Average diameters (with standard deviation) of nanofibers in standard ENM recipes (Table 1). Fiber diameters were measured from SEM images using ImageJ software. Typically, 100 nanofiber diameters were measured per ENM sample, allowing size distributions to be calculated for all synthesized materials. n = number of replicate syntheses.	20
Table 6. Summary of ENM-water equilibrium partition coefficients [average and standard deviation as $\log(C_m/C_w)$ in L/kg] for aniline and nitrobenzene (NM = not measured).	24
Table 7. Summary of ENM-water equilibrium partition coefficients [average and standard deviation as $\log(C_m/C_w)$ in L/kg] for selected PCB congeners and dioxin.	26
Table 8. Partition coefficients [average and standard deviation as $\log(C_m/C_w)$ in L/kg] for aniline and nitrobenzene using ENM integrated with CNTs (NM = not measured).	31
Table 9. ENM-water equilibrium partition coefficients [as $\log(C_m/C_w)$ in L/kg] for selected PCB congeners and dioxin for PS-ENM amended with CNTs.	32

List of Figures

Figure 1. Schematic of an electrospinning apparatus, including high-voltage power supply, spinneret (metallic needle), collector (aluminum foil or metallic drum) and syringe pump.	6
Figure 2. Images collected across a range of scales for a polystyrene ENM. The images highlight the dual character of ENMs, where a robust bulk structure (i.e., nonwoven mats) consists of fibers within the nanodomain.	7
Figure 3. Laboratory scale electrospinning apparatus used to fabricate all ENMs tested herein. ..	8
Figure 4. Polymers used in the synthesis of our electrospun nanofiber mats (ENMs).	9
Figure 5. Chemical structure of SDS and TBAB surfactants.	11

Figure 6. PAN hydroxylamine reaction.....	11
Figure 7. Schematic of our multilayer ENMs. The left panel shows a “two” layer ENM consisting of PMMA and PS. Right panel shows a “tri” layer ENM consisting of PS, PMMA and PS.....	12
Figure 8. Diagram flow of the uptake and partition coefficient experiments for aniline and nitrobenzene.....	14
Figure 9. Images of polymer ENMs fabricated herein. ENM receipts are shown in Table 1.....	19
Figure 10. Histogram examples of four batches of PS-ENM fabricated over one-year SEED project. Diameters for at least 100 individual nanofibers within ENMs were quantified via SEM to produce these distributions.	20
Figure 11. Histogram examples of three batches of PS-ENM fabricated as a function of relative humidity. Relative humidity could be used to tailor average diameter, with size distributions decreasing with relative humidity. Diameters for at least 100 individual nanofibers within ENMs were quantified via SEM to produce these distributions.	21
Figure 12. Influence of sol gel volume on the thickness (in mm) of PAN and PAN with TBAB ENMs. ENM thickness was quantified from cross-sectional SEM, with representative images shown.	22
Figure 13. Photographs illustrating the handling, manipulation and mechanical strength of a representative PS-ENM.	23
Figure 14. Picture of bulk PS-ENM (left) and a PS-ENM composite after integration of carbon nanotubes (CNTs).....	23
Figure 15. Diameter size distributions for PAN and PAN amended with three different loadings of the cationic surfactant TBAB (0.5, 1 and 2% by weight). Mean diameters (with standard deviation) are: 120 ± 40 nm for PAN; 130 ± 30 nm for TBAB0.5; 130 ± 40 nm for TBAB1; and 130 ± 30 nm for TBAB2.	24
Figure 16. ENM uptake curves for aniline (left panel) and nitrobenzene (right panel) for our different ENMs. The error bars represent the standard deviation from two different uptake experiments. Laboratory set up: pH ~ 6.5 (DI water), initial aniline and nitrobenzene concentrations 25 μ M (aniline: 2 mg/L, nitrobenzene: 3 mg/L), ENM loading ~1.5 g/L. PAN-ENM, PS-ENM and PMMA-ENM). PAN, PMMA are hydrophilic ENMs; PET, PS and PVDF are hydrophobic; and EVA has both chemical groups.....	25
Figure 17. ENM uptake curves for selected PCB congeners and dioxin (TCDD). The error bars represent the standard deviation from two different uptake experiments. Laboratory set up: pH ~ 6.5 (DI water), initial concentrations from 0.25 to 5 ng/L, ENM loading ~3 g/L.	27
Figure 18. ENM-water equilibrium partition coefficients (L/kg) for aniline (AN) and nitrobenzene (NB) were measured changing the aqueous pH for PS-ENM and PMMA-ENM. .	

Laboratory set up: initial aniline and nitrobenzene concentrations 25 μM (aniline: 2 mg/L, nitrobenzene: 3 mg/L), ENM loading ~ 1.5 g/L. Experiments were performed for 5 days. pH was controlled using commercially available buffers (MES, HEPES, AMPSO and BioXtra). 28

Figure 19. Sorption isotherm using PS-ENM and PMMA-ENM for aniline (left panel) and nitrobenzene (right panel). Initial aqueous concentrations varied from 10 to 200 μM (aniline: 1 - 19 mg/L, nitrobenzene: 1 – 25 mg/L). The error bars represent the standard deviation from two different uptake experiments. Laboratory set up: pH ~ 6.5 (DI water), and ENM loading ~ 1.5 g/L. Experiments were performed for 5 days. 29

Figure 20. ENM uptake curves for aniline (left panel) and nitrobenzene (right panel) for modified CNT ENMs. The error bars represent the standard deviation from two different uptake experiments. Laboratory set up: pH ~ 6.5 (DI water), initial aniline and nitrobenzene concentrations 25 μM (aniline: 2 mg/L, nitrobenzene: 3 mg/L), ENM loading ~ 1.5 g/L. 31

Figure 21. ENM uptake curves for aniline (left panel) and nitrobenzene (right panel) for surfactants and amidoximated modified PAN-ENMs. Laboratory set up: pH ~ 6.5 (DI water), initial aniline and nitrobenzene concentrations 25 μM (aniline: 2 mg/L, nitrobenzene: 3 mg/L), ENM loading ~ 1.5 g/L. 33

Figure 22. ENM uptake curves for aniline (circle) and nitrobenzene (triangle) for silver nanoparticles modified PAN (panel a) and PS (panel b) ENMs. Laboratory set up: pH ~ 6.5 (DI water), initial aniline and nitrobenzene concentrations 25 μM (aniline: 2 mg/L, nitrobenzene: 3 mg/L), ENM loading ~ 1.5 g/L. 34

Figure 23. Summary of the ENM-water equilibrium partition coefficients for aniline obtained from all the ENMs synthesized. Commercially available materials were also included such as PS beads, PDMS fiber and LDPE film. 36

Figure 24. Summary of the ENM-water equilibrium partition coefficients for nitrobenzene obtained from all the ENMs synthesized. Commercially available materials were also included, such as PS beads, PDMS fiber and LDPE film. 36

Figure 25. Summary of the ENM-water equilibrium partition coefficients for PCB47 (left panel) and dioxin (right panel) obtained from the four ENMs synthesized, modified ENMs with CNTs and from modeled partition coefficients from commercially available materials, such as POM film, SPME (PDMS fiber) and LDPE film (1, 61). 37

Figure 26. Laboratory pore water measurements of nitrobenzene from our model spiked soil using PS, PMMA, PS-CNT (functionalized) and PS-PMMA-PS ENMs. Lines are drawn as guide to the eye. 38

Figure 27. Photograph sequence of cleaning PS-ENM after being exposed to model soil experiments. 39

Figure 28. Laboratory pore water measurements of aniline from our model spiked soil using PS-PMMA-PS ENMs. Lines are drawn as guide to the eye. 40

Figure 29. Sediment pore water concentration measurements in pg/L carried out using PS-ENM and PMMA-ENM. 30 grams of wet sediment from IHSC with ENMs were tumbled for 50 days.
..... 41

List of Acronyms

AN: Aniline
CNT: Carbon nanotubes
DCM: Dichloromethane
DI: Deionized Water
Dioxin: 2,3,7,8-Tetrachlorodibenzodioxin
DMA: N,N-Dimethylacetamide.
DMF: Dimethylformamide
DOD: Department of Defense
ENM: Electrospun nanofiber mat
EVA: Ethylene-vinyl acetate
GAA: Glacial Acetic Acid
GC-MS/MS: Gas chromatography coupled to tandem mass spectrometry
 K_D = Equilibrium partition coefficient
Kow: Octanol-water partition coefficient
LC/DAD: Liquid chromatography with diode array detection
LDPE: Low density polyethylene
NB: Nitrobenzene
PAN: Polyacrylonitrile
PCB: Polychlorinated biphenyl
PDMS: Polydimethylsiloxane
PET: Polyethylene terephthalate
PMMA: Polymethylmethacrylate
POM: Polyoxymethylene
PS: Polystyrene
PVAc: Poly(vinyl acetate)
PVDF: Polyvinylidene fluoride
QA/QC: Quality assurance and control
RSD: Relative standard deviation
SDS: Sodium dodecyl sulfonate
SEM: Scanning electron microscopy
SPME: Solid phase microextraction
TBAB: Tetrabutylammonium
TFA: Trifluoroacetic acid

Keywords

Electrospinning, hydrophilic and hydrophobic compounds, sediment pore water, passive sampling materials

Acknowledgements

We would like to thank SERDP W912HQ-15-P-0022, Iowa Superfund Research Program NIH P42 ES013661, and USEPA grant RD835177. At the University of Iowa, we thank our laboratory director Eric Jetter for his help in the laboratory.

Abstract

Objectives: The principal objective of this project was to develop new and innovative nanomaterials to overcome traditional hurdles in existing passive sampling devices (e.g., multi-target sampler for chemically diverse compounds), thereby improving the Department of Defense's (DOD) ability to characterize the distribution and concentrations of pollutants at their contaminated sites.

Technical Approach: Using electrospinning, we synthesized seven electrospun nanofiber mats (ENMs) from polymers [ethylene-vinyl-acetate (EVA), polyacrylonitrile (PAN), polyethylene terephthalate (PET), polymethylmethacrylate (PMMA), polystyrene (PS), polyvinyl acetate (PVAc) and polyvinylidene fluoride (PVDF)] and investigated their performance as next-generation passive sampling materials. Given the ease of material fabrication provided by electrospinning, we were able to tune the physical and chemical properties of polymeric ENMs to produce robust materials with improved selectivity and enhanced sorption capacities toward several DOD relevant target pollutants. We tested ENM performance in homogeneous (i.e., single phase) aqueous systems as well as heterogeneous (i.e., dual phase) systems containing model soils against targets including aniline and nitrobenzene (as models for TNT and RDX) and a selection of ten PCB congeners and dioxin. These chemical targets were selected because of their wide range of physical-chemical properties (e.g., $\log K_{ow}$ values spanning 8 orders of magnitude) and relevance as polar munitions constituents and hydrophobic compounds commonly encountered at contaminated DOD sites.

Results: Generally, aqueous uptake experiments with ENMs revealed very fast rates of partitioning with equilibration times less than 1 d. Equilibrium partition coefficients (L/kg) for ENMs ranged from 0.72 to 2.8 log units for aniline and nitrobenzene, with evidence suggesting uptake via partitioning into the bulk nanofiber (i.e., absorption) and specific binding interactions (e.g., hydrogen-bonding and Coulombic interactions) contributing to, and potentially controlling, polar target uptake. PCBs and dioxin also exhibited very fast equilibrium uptake (achieved in < 18 h), with equilibrium partition coefficients for ENMs ranging from 3.2 to 6.4 log units. Collectively, the rates and partition coefficients measured for the best performing ENMs often exceeded partition coefficients achieved with commercially available passive sampling materials (e.g., low-density polyethylene and PDMS glass fiber), particularly for polar analytes. Across a range of experimental conditions (e.g., variable pH, analyte concentration, and complex analyte mixtures), little change in ENM performance was observed. We also found promising performance in heterogeneous systems with model soils, where the optimal ENM, polystyrene, not only yielded reproducible measurement of nitrobenzene pore water concentration but also allowed for greater ease of handling by minimizing unwanted polymer-soil organic matter interactions. Building upon these promising results, further efforts improved performance through fabrication of novel polymer composites and surface-chemical functionalized ENMs. For example, we demonstrate that carbon nanotubes functionalized with carboxylic acid functional groups (which are deprotonated at pH 7) or the inclusion of anionic surfactants could be used to promote uptake of aniline (by as much as 1 log unit in partition coefficient), a fraction of which is positively charged under our experimental conditions. Further, integration of silver nanoparticles with select ENMs can be used to impart biocidal activity, thereby slowing biofouling during application. We also fabricated novel multilayer ENMs, in which layer-by-

layer combinations of different polymers impart multi-target capabilities (e.g., simultaneous uptake of polar and hydrophobic species) and greater ease of application and handling in complex media (e.g., protective surface layers that limit fouling).

Benefits: Overall, our results support our initial hypothesis that electrospun nanofiber mats represent next-generation passive sampling materials that can be easily modified to enhance compound selectivity, sorption capacities and improve field applications. Tangible deliverables include (i) recipes for the synthesis of a suite of polymer ENMs with tunable physical and chemical properties that can be exploited to optimize their performance as sorbents; (ii) analytical methods, including laboratory protocols, for the application and extraction of polymer ENMs in complex media, including sediments and pollutant mixtures; and (iii) recommendations for further optimizing the application and performance of ENMs in complex media and for pollutant mixtures. Ultimately, this SEED project will serve to catalyze the production of innovative nanoenabled materials with the potential to expand the use and increase the reliability and performance of passive sampling devices. This may in turn lead to improved site characterization, where the small ENM material footprint should allow better spatial resolution of data and their fast rates of uptake should enable better temporal resolution of data. Further, there is great potential for the rapid scale up and transition of this technology to the commercial marketplace because electrospinning is already an industrially viable fabrication process for non-woven polymers. Ultimately, these outcomes also pave the way for future research that will examine a broader suite of DOD relevant chemicals, aim to further enhance ENM capacity, selectivity, and functionality, and scale-up and prototype an ENM-based passive sampler for field deployment and testing.

Objective

The principal objective of this project was to develop new and innovative nanomaterials to overcome traditional hurdles in existing passive sampling devices (e.g., multi-target sampler for chemically diverse compounds), thereby improving the Department of Defense's (DOD) ability to characterize the distribution and concentrations of pollutants at their contaminated sites. Accordingly, this **proof-of-concept** project aimed to fabricate polymers as electrospun nanofiber mats (ENMs) that can be used as passive sampling materials to measure simultaneously hydrophilic ($\log K_{ow} < 3$) and hydrophobic ($\log K_{ow} > 4$) targets at DOD contaminated sites. Further, by exploiting the ease of material fabrication afforded by electrospinning, we aimed to selectively tailor the physical and surface/bulk chemical properties of ENMs to not only enhance their uptake rate and capacity toward diverse, DOD-relevant chemical targets, but also improve practical aspects associated with their application and handling in complex field environments.

Specific research objectives were to:

- **Objective 1:** Synthesize and characterize a suite of polymer ENMs via electrospinning for use as sorbent materials in passive samplers targeting both hydrophilic and hydrophobic pollutants;
- **Objective 2:** Determine the equilibrium partition coefficients for each of the ENMs through laboratory experiments in homogeneous (aqueous) systems with a set of pollutant targets including aniline (AN) and nitrobenzene (NB) (as models for TNT and RDX), as well as polychlorinated biphenyl (PCB) congeners and 2,3,7,8-tetrachlorodibenzodioxin (dioxin);
- **Objective 3:** Optimize the performance of the most promising polymer ENMs by tailoring their physical, chemical and material properties during electrospinning, while also fabricating multilayer ENMs ideal for the simultaneous analysis of chemically diverse pollutant targets (e.g., hydrophobic and hydrophilic pollutant classes); and
- **Objective 4:** Evaluate the performance of optimal polymer ENMs toward the aforementioned pollutant classes in heterogeneous (i.e., two-phase) systems containing either model soils or anthropogenically impacted sediments.

In addressing these objectives, criteria for success of the SEED project were established as follows:

- **Criteria 1:** Protocols (i.e., recipes), supported by direct experimental evidence and material characterization, for the reproducible synthesis of physically and chemically tailored polymer ENMs.
- **Criteria 2:** Experimentally measured ENM-water partition coefficients for hydrophilic and hydrophobic pollutant classes that are on par with or exceed those measured or previously reported for commercially available passive sampling materials.

- **Criteria 3:** Reliable and reproducible application of polymer ENM materials in complex, environmentally relevant systems, including pollutant mixtures and contaminated soil and sediment.

To date, we have executed an experimental plan that successfully achieved each of these objectives and met each of the established criteria for project success. In doing so, we have acquired sufficient proof-of-concept data to eliminate most risks associated with any further research and development related to these innovative materials. Indeed, tangible outcomes and deliverables of this SEED project that can serve as the foundation for future investigations into the application of ENM-based passive sampling devices include:

- Recipes for the synthesis of a suite of polymer ENMs with tunable physical and chemical properties that can be exploited to optimize their performance as sorbents.
- Analytical methods, including laboratory protocols, for the application and extraction of polymer ENMs in complex media, including sediments and pollutant mixtures.
- Best practices for further optimizing the application and performance of ENMs in complex media (e.g., biocidal materials to slow fouling) and for pollutant mixtures (e.g., multilayer structures for simultaneous targeting of diverse chemical classes).

Finally, the overarching implications and outcomes of this SEED project include:

- Development of innovative nanoenabled materials with the potential to expand the use and increase the reliability and performance of passive sampling devices.
- The potential for improved site characterization via small ENM material footprint that should allow better spatial resolution of data, while fast rates of uptake will allow for better temporal resolution of data.
- The potential for rapid scale up and transition of this technology to the commercial marketplace because electrospinning is already an industrially viable fabrication process for non-woven polymers.

These SEED project outcomes directly respond to the FY 2015 SERDP Exploratory Development (SEED) Statement of Need (SON) “Development of Passive Sampling Methodologies to Measure Contaminant Bioavailability in Aquatic Sediments” (ERSEED-15-02). Under ERSEED-15-2, the need to develop a passive sampling methodology for munition constituents, as well as dioxins/furans and PCBs, was explicitly stated, and these were the target contaminants of this exploratory research investigation. Further, this SEED project developed and evaluated the performance of several ENMs that due to their nanoscale dimensions represent a significant step forward in passive sampling technology development for sediment pore waters and the water column. Specifically, ENMs hold of the promise of (i) integration of multiple polymer layers into a single passive sampling device for the simultaneous measurement of diverse pollutant classes; (ii) high surface-area-to-volume ratio for greater rates of uptake to improve temporal resolution of data collection; and (iii) a small device footprint for improved spatial resolution of data collection. Accordingly, we contend our results are of the highest relevance to SERDP and SEED SON ERSEED-15-02; they provide an innovative and promising solution for challenges that have long hindered the ability of DOD to fully characterize sites contaminated by complex mixtures of persistent and emerging pollutant classes.

Background

Opportunities in Passive Sampler Development

The DOD is responsible to environmentally restore and close all of their sites with contaminated sediments. A diverse suite of organic contaminants exhibiting a wide range of chemical properties, toxicities, and concentrations are present at these sites. These include hydrophilic compounds such as munitions constituents (e.g., TNT and RDX) and their metabolites (e.g., ADNTs, DANTs and TNX), as well as hydrophobic compounds including pollutant classes like dioxins and PCBs.

Accurately measuring the abundance of these pollutant classes, especially in the freely dissolved sediment pore water and surficial water phases, is critical to the effective management of contaminated sites but not a trivial task given system complexity. For this purpose, use of passive sampling devices has increased remarkably over the last decade, particularly for the determination of the freely dissolved sediment pore water and surficial water concentrations of hydrophobic organic contaminants (e.g., see references 1-5). To date, however, much less attention has focused on the development of passive samplers for hydrophilic contaminants (e.g., see references 5-11). In a noteworthy example, Alvarez *et al.* (7) were among the first to develop and field deploy (for 56 d) passive samplers operating in the linear uptake stage for measurement of polar compounds in surface water (the so-called Polar Organic Chemical Integrative Samplers, or POCIS). They focused on organic compounds with values of $\log K_{ow} < 4$, with field results for two herbicides and a naturally occurring hormone yielding good agreement with conventional sampling methods. Metcalfe *et al.* (10) also used the POCIS sampler to measure the presence of selected pharmaceuticals and other polar compounds in drinking water. Their results were mostly consistent with measurements from corresponding grab samples.

Nevertheless, critical gaps in these and other existing passive sampling devices exist that may ultimately limit their applicability to the mixtures of contaminants most relevant to DOD. These limitations, mainly for the hydrophilic polar samplers, are both fundamental and practical in nature, including:

- Lack of understanding of uptake kinetics and sorption mechanisms of polar compounds on traditional sorbent materials. Currently, there are no theoretical models able to predict accurately the uptake of polar targets based on their physicochemical properties, including K_{ow} values, Hansen solubility parameters, or water solubility (5, 10, 12-14). This problem is particularly important for passive samplers that operate in the kinetic uptake regime and yield a time-weighted average concentration (i.e., integrative passive sampler), where a sampling rate has to be determined either by laboratory or field calibrations to calculate environmental exposure;
- Uncertainty regarding the use of performance reference compounds (PRCs) for estimating sampling rates. This uncertainty comes from the insufficient information on the sorption mechanisms involved in the uptake of hydrophilic compounds into passive samplers for such targets (e.g., POCIS) (13, 14);
- Loss of sorbent material during long deployments. This is particularly problematic for POCIS samplers, which can potentially reduce the active sorbent media available during application (11);

- Even though POCIS is supposed to operate in the uptake kinetic mode, decreasing concentrations of certain pollutants have been detected over time, suggesting that there are instances where it may operate in the equilibrium regime (10); and
- Influence of field conditions on the performance of passive samplers for hydrophilic and hydrophobic compounds, many of which have not been described quantitatively. For example, biofouling still complicates their performance (e.g., uptake ability) and interpretation of the data collected from these samples (5, 6).

Electrospun Nanofiber Mats as a Next-Generation Passive Sampling Platform

Our scientific approach utilizes the innovative material fabrication technique of electrospinning to synthesize electrospun nanofiber mats (ENMs) for use as passive sampling materials (**Figure 1**).

Electrospinning is a process for fabricating non-woven mats of nanofibers (or microfibers) by forcing a conductive polymer sol-gel or melt through a metal nozzle and drawing a solution droplet to form fibers under the force of an applied electric field. Briefly, a high voltage is applied to the syringe needle while the collector is grounded. The conductive polymer sol-gel is then pushed out from the syringe at a steady flow rate, driven by the electric field between needle and collector. The sol-gel forms a Taylor Cone on the needle tip and is then dispersed uniformly to generate the nanofibers. The final product is a robust, non-woven mat constructed of polymer nanofibers. Because of its simplicity (15) and high productivity (16), electrospinning has been widely used in both academia and industry, where several advantages of polymer nanofibers have been discovered across a range of applications (17, 18).

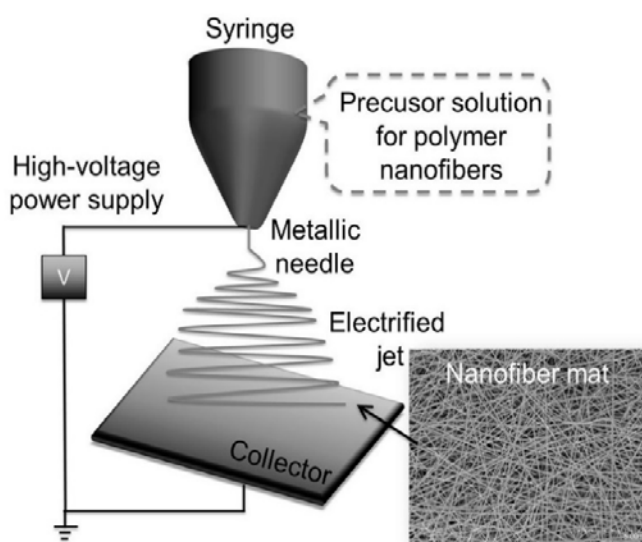


Figure 1. Schematic of an electrospinning apparatus, including high-voltage power supply, spinneret (metallic needle), collector (aluminum foil or metallic drum) and syringe pump.

To the best of our knowledge, this SEED project is the first demonstration of such materials for use in passive sampling devices, expanding upon their more traditional applications in biomedicine (e.g. drug delivery, tissue engineering), functional materials and devices (e.g. clothing and smart textiles), and energy and electronics (e.g. batteries/cells and capacitors) (19). We contend that the use of electrospinning to fabricate polymer sorbents for use as passive sampling materials will catalyze a new era in environmental sampling because:

- ENMs possess a high surface area-to-volume ratio. Nanofiber diameters can be tuned during synthesis to yield typical dimensions between 50 nm to 300 nm and uniform

diameter distributions. Thus, ENMs can possess nanoscale properties (i.e., nanoscale is typically defined as having one characteristic dimension less than 100 nm) in a robust, bulk structure (i.e., a nonwoven nanofiber mat) with reliable mechanical strength (**Figure 2**) (20). The large surface area-to-volume ratio confers many favorable physical and chemical properties to ENMs (21), particularly for interfacial processes like adsorption or absorption where greater rates and capacity for partitioning can be anticipated per unit mass of material.

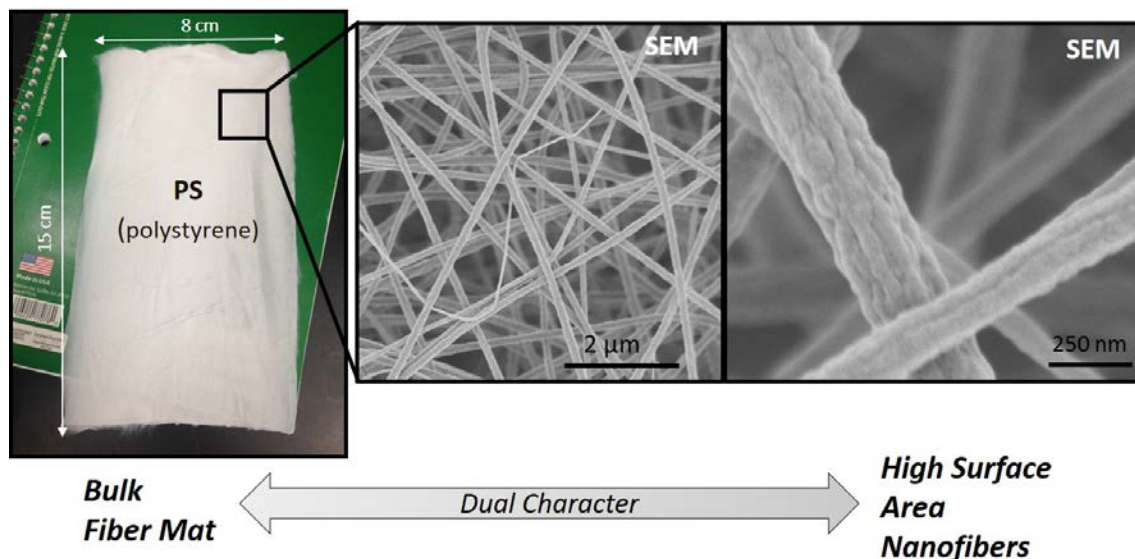


Figure 2. Images collected across a range of scales for a polystyrene ENM. The images highlight the dual character of ENMs, where a robust bulk structure (i.e., nonwoven mats) consists of fibers within the nanodomain.

- ENM properties are tunable by controlling synthesis variables. Electrospinning affords exquisite control of nanofiber physical and chemical properties, while ENMs are also highly amenable to modification post-production. Thus, as a fabrication platform, it is highly versatile and allows material properties to be tailored to specific ENM endpoint applications (17, 22, 23).
- A range of chemically diverse polymers, as well as polymer composites, can be fabricated via electrospinning. The requirement is solely that precursors for all targeted materials be dissolved into a compatible solvent. To date, hundreds of materials including metals, metal oxides, and polymers have been used to produce ENMs for various applications, from biomedical to environmental (19).
- Electrospinning is a proven and reliable approach for fabrication of nanostructured materials. Accordingly, it is a process that is highly scalable and already industrially viable for a range of nonwoven material applications (24). Recipes for promising materials developed as part of this SEED grant can easily be scaled and prototyped to promote rapid translation of technology into the commercial market place (25-28).

As demonstrated in this SEED project, these advantages of electrospinning enable ENMs to perform well as passive sampling materials (e.g., they outperform current commercially available

passive sampling materials), while also providing several avenues by which ENMs can be further tailored and modified to improve their performance and functionality for *in situ* measurements.

Material and Methods

Synthesis of Electrospun Polymer Nanofiber Mats (ENMs)

ENMs were synthesized using a custom electrospinning rig constructed in the Cwiertny laboratory (**Figure 3**). Operationally, the selected polymer was dissolved into a suitable organic solvent and transferred into a syringe with a metal needle, to which a high voltage was applied. The electrospinning solution was ejected from the blunt needle tip under a strong electric field (up to several kV per cm), and the nanofiber mat was collected on a grounded drum collector wrapped in Al foil. Nanofiber diameters were adjusted between ~100-200 nm by controlling the electrospinning solution (e.g., viscosity, dielectric constant, electrical conductivity, and surface tension), electrospinning parameters (e.g., flow rate, applied voltage, distance between collector and spinneret, rotation rate of drum collector), and environmental factors (e.g., temperature, humidity).

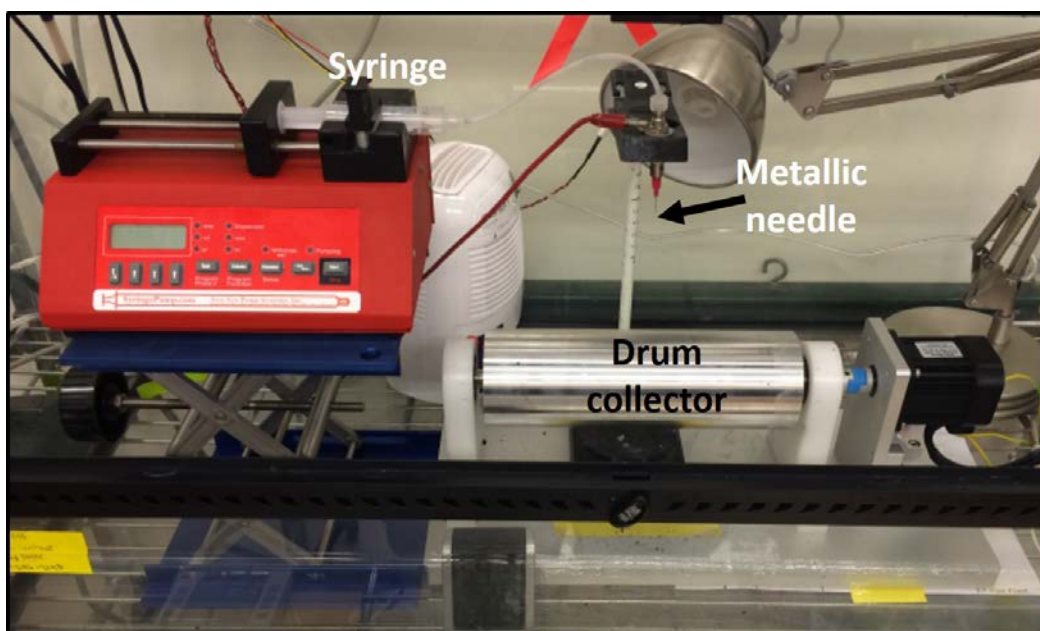


Figure 3. Laboratory scale electrospinning apparatus used to fabricate all ENMs tested herein.

Seven polymer ENMs were synthesized (**Figure 4**). Due to the different physical and chemical properties of the pollutant targets to be tested, we investigated the performance of three hydrophilic and three hydrophobic polymers, as well as a co-polymer (possessing both hydrophilic and hydrophobic moieties) that has previously been used in passive sampling applications (9).

Figure 4. Polymers used in the synthesis of our electrospun nanofiber mats (ENMs).

We note that in our original proposal, we also intended to fabricate polyoxymethylene (POM) ENMs. However, all recipes for the production of POM nanofibers required aggressive chemical reagents (e.g., hexafluoro-2-propanol), which would likely render their scale up and commercial development impractical. Thus, we elected to conduct experiments with polyvinylidene fluoride (PVDF) as an alternative, more easily synthesized, hydrophobic polymer.

For the fabrication of each polymer ENM, synthesis recipes were adapted from established protocols in the literature (18, 29-39), with key reagents and parameters summarized in **Table 1**. For example, synthesis of polystyrene (PS) ENMs involved the dissolution of commercial polystyrene beads into N,N-dimethylformamide at 60 °C. This mixture was stirred for 2 h, creating a homogenous and clear sol-gel with a typical PS concentration of 10% (w/v). The PS sol-gel was transferred into a 12 mL syringe, which was then mounted on a syringe pump. A 25G plastic needle was used to expel the polymer solution, with the needle tip connected to a high-voltage (up to 30 kV) power supply. During synthesis, the flow (pump) rate of the polymer sol-gel from the syringe was 0.3 mL/h, while the needle-tip voltage was 17 kV. A grounded, rotating metal drum collector (covered with Al foil) was used to collect deposited ENMs, with the distance between the collector and needle tip fixed at 10 cm. All electrospinning was conducted under a controlled environment within a custom environmental chamber, where temperature and humidity were fixed at a desired value between 20 °C to 28 °C and 16% to 20%, respectively.

Table 1. Reagents, physical and chemical properties, and electrospinning synthesis parameters for ENMs investigated herein.

Reagent Details	PAN	PS	PMMA	PVAc	PET	PVDF	EVA
Solvent (v/v)	DMF	DMF	5:1 DMF: GAA	3:1 GAA: DI water	1:1 DCM:TFA	25:9 Acetone : DMA	5:3 DCM : DMF
Polymer to solvent ration (w/w)	0.087	0.11	0.071	0.25	0.071	0.14	0.053
Polymer weight (%)	8	10	6.6	20	6.6	12	5
Physical and Chemical Properties of ENMs*							
Monomer	(C ₃ H ₃ N) _n	(C ₈ H ₈) _n	(C ₅ O ₂ H ₈) _n	(C ₄ H ₆ O ₂) _n	(C ₁₀ H ₈ O ₄) _n	(C ₂ H ₂ F ₂) _n	(C ₂ H ₄) _n (C ₄ H ₆ O ₂) _m
O or N content (w %)	26	0	32	37	33	0	$\frac{800m}{35m + 7n}$
Density (g/cm ³)	1.2	1.0	1.2	1.2	1.4	1.8	1.0
Glass transition temperature (°C)	95	100	105	30	70 (amorphous) 80 (crystalline)	-35	-40
Electrospinning Synthesis Parameters							
Distance needle-collector (cm)	10	10	10	10	10	10	25
Voltage (kV)	13	17	9	16	16	22	23
Pump flow (mL/h)	0.5	0.3	0.3	0.3	0.4	0.7	2
Needle gauge size	25G	25G	25G	25G	23G	25G	18G
References from which recipes were adapted	(38)	(30, 32)	(36)	(31, 34)	(18, 37)	(29, 33)	(35, 39)

DMF: Dimethylformamide; GAA: Glacial Acetic Acid; DCM: Dichloromethane; TFA: Trifluoroacetic acid; DMA: N,N-Dimethylacetamide. *All the polymer monomers are insoluble in water.

Preparation of Chemically Modified ENMs and ENM Composites

Several approaches were used to increase ENM functionality through integration of other reagents that could impart desirable physical or chemical properties. These included:

- Integration of cationic and anionic surfactants to alter the surface charge of the resulting ENMs;
- Integration of carbon nanotubes (CNTs) to provide additional binding sites for pollutant uptake as well as increasing ENM material strength;
- Post-synthesis chemical functionalization of ENMs to introduce specific binding sites on the ENM surface; and
- Integration of biocidal silver (Ag) nanoparticles to decrease ENM biofouling during application.

Electrospinning allowed for the facile synthesis of these modified materials, where in most cases key reagents could be mixed into the precursor sol gel solution prior to electrospinning. Indeed, a major benefit of ENMs is the ease with which multi-component or composite materials can be fabricated, simply by uniformly mixing material building blocks into the precursor solution that is ultimately loaded into the syringe for electrospinning.

For fabrication of surfactant modified ENMs, PAN was blended with either the anionic surfactant sodium dodecyl sulfonate (SDS) or the cationic surfactant tetrabutylammonium bromide (TBAB) (**Figure 5**) at a ratio of 1:100 (w/w) and then this mixture was transferred to the syringe for electrospinning. Similarly, silver (Ag) nanoparticles (Sigma-Aldrich; 20 nm particle size) were mixed with PS and PMMA at a 1:3 (w/w) to produce biocidal ENMs. For CNT-composites, PS was mixed with either functionalized (i.e., with COOH surface sites) or non-functionalized (i.e., as received) commercial CNTs purchased from CheapTubes (www.cheaptubes.com). For these composites, CNTs were loaded into the electrospinning sol gel at either 20 or 30% (w/w).

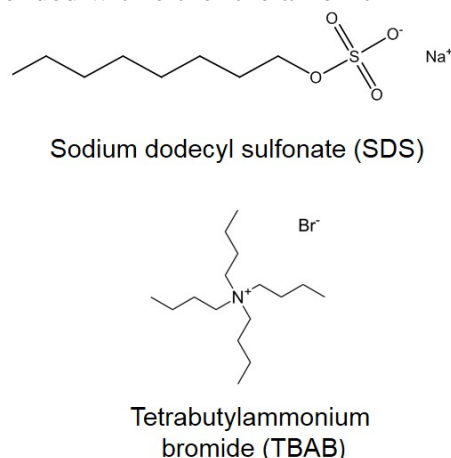


Figure 5. Chemical structure of SDS and TBAB surfactants.

To produce surface functionalized ENMs with various O and N-based binding sites, PAN ENMs were reacted with hydroxylamine (**Figure 6**) after electrospinning. This produces amidoxime sites on the ENM surface (40). These sites are electron rich (through lone pairs available on surface N and O groups), and thus may promote uptake of more polar analytical targets that partition through specific binding interactions including

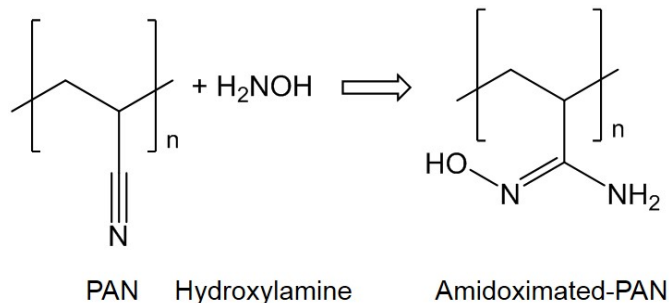


Figure 6. PAN hydroxylamine reaction.

hydrogen bonding or electron donor-acceptor interactions.

Preparation of Multilayer ENMs

In addition to individual or single-layer ENMs, bi-layer and tri-layer ENMs were also fabricated using different polymer combinations (**Figure 7**). The multilayer materials fabricated include PAN-PS, PAN-EVA, PS-EVA, and PS-PMMA-PS, and these were explored to examine for potential synergies in multi-polymer applications (e.g., simultaneous targeting of different pollutant classes with different chemically active polymers). To produce these innovative multilayer structures, polymers were electrospun in series, resulting in layer-by-layer growth on the grounded collector. Thus, these multilayered ENMs are a single unit, but possess distinct phases of each polymer and are not a homogeneous co-polymer blend.

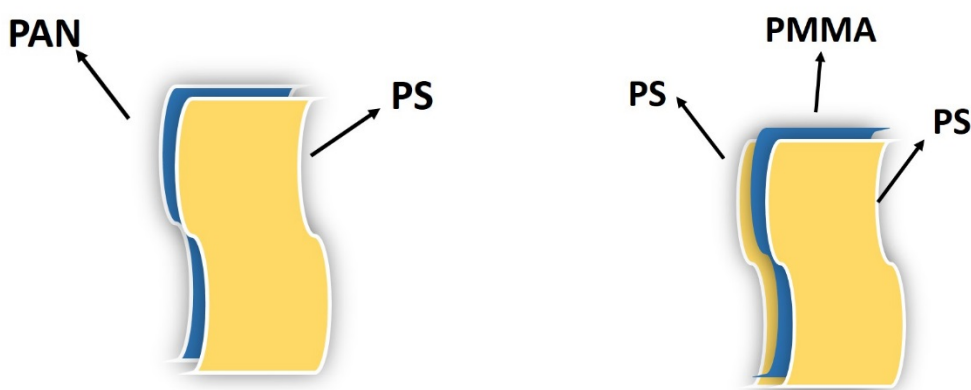


Figure 7. Schematic of our multilayer ENMs. The left panel shows a “bi-layer” ENM consisting of PAN and PS. The right panel shows a “tri-layer” ENM consisting of PS, PMMA and PS.

ENMs Characterization, Stability and Strength Testing

ENMs were characterized extensively for their physical, chemical and material properties. ENM morphology was evaluated via scanning electron microscopy (SEM). Fiber diameters were measured from SEM images using ImageJ software (version 1.51a; available at <https://imagej.nih.gov/ij/index.html>). Typically, 100 nanofiber diameters were measured per ENM sample, allowing size distributions (with mean diameter and standard deviation) to be calculated for all synthesized materials.

Another important consideration is the stability of ENMs during application in passive sampling devices and subsequent analytical processing (e.g., solvent extraction). Accordingly, we tested the stability of various ENMs in water across a range of pH values (from 2-12) to mimic solution conditions representative of their deployment in a passive sampling device. We also tested their stability in organic solvents (e.g., methanol, acetonitrile, acetone) commonly used in laboratory analytical processing of passive sampling materials for extraction of sorbed constituents.

Finally, the mechanical strength of ENMs was evaluated by stress-strain curves developed using a load-displacement cell, as described in detail in our recent work (41). Briefly, stress-strain

curves were developed for select ENMs from load-displacement data collected with a BioTense Perfusion Bioreactor (ADMET, Inc., Norwood, MA), which consisted of a linear actuator, sample grips, a reactor frame, and a 250 g load cell. Using this set-up, the Young's modulus of ENMs could be calculated from the slope of the stress-strain curves. Further, the ultimate tensile stress (UTS) and ultimate strain could be calculated from the curve as the highest stress achieved before specimen failure and the corresponding strain, respectively.

Target Analytes

Table 2 shows the analytes (i.e., target dissolved pollutants) used in this study, along with select physicochemical properties including aqueous solubility and octanol-water partition coefficients (or $\log K_{ow}$ values). One particular emphasis was polar targets, where we focused on aniline and nitrobenzene as model compounds for common munition constituents of interest to DOD (42). For example, $\log K_{ow}$ values for nitrobenzene and aniline are comparable to those of TNT ($\log K_{ow} = 1.6$), RDX ($\log K_{ow} = 0.90$), as well as their metabolites including 2-ADNT ($\log K_{ow} = 1.9$) and TNX ($\log K_{ow} = 0.52$). Moreover, beyond simple comparisons of $\log K_{ow}$ values, our model compounds share many of the same functional groups (e.g., R-NH₂) that may participate in specific binding interactions critical to uptake of these targets into passive sampling materials.

Beyond these polar model analytes, we also included hydrophobic pollutant classes including dioxin and a suite of PCB congeners. These were chosen for their ubiquity in sediments at contaminated sites (43-45). Given their considerable differences in solubility and $\log K_{ow}$ value relative to the aforementioned polar targets, these also give us a complementary set of analytes to explore for development of a multi-target passive sampling device (i.e., simultaneous and non-competitive uptake of diverse pollutant classes across a range of $\log K_{ow}$ values).

Table 2. Name and select physicochemical properties of the analytes (i.e., pollutant targets) investigated herein. Sources of data are listed in parenthesis.

Analyte	Common name	CAS number	Water solubility (mg/L)	$\log K_{ow}$
Phenylamine	Aniline	62-53-3	33800 (46)	0.9 (47)
Nitrobenzene	Nitrobenzene	98-95-3	2100 (46)	1.9 (47)
2-Chlorobiphenyl	PCB1	2051-60-7	4.8 (48)	4.5 (49)
3,3'-Dichlorobiphenyl	PCB11	2050-67-1	0.61 (48)	5.3 (49)
2,4,5-Trichlorobiphenyl	PCB29	15862-07-4	0.22 (48)	5.6 (49)
2,2',4,4'-Tetrachlorobiphenyl	PCB47	2437-79-8	0.07 (48)	5.9 (49)
2,3',4,5',6-Pentachlorobiphenyl	PCB121	56558-18-0	0.026 (48)	6.6 (49)
2,2',3,3',6,6'-Hexachlorobiphenyl	PCB136	38411-22-2	0.027 (48)	6.2 (49)
2,2',3,4',5,5',6-Heptachlorobiphenyl	PCB187	52663-68-0	0.009 (48)	7.2 (49)
2,2',3,3',4,4',5,5'-Octachlorobiphenyl	PCB194	35694-08-7	0.001 (48)	7.8 (49)
2,2',3,3',4,4',5,5',6-Nonachlorobiphenyl	PCB206	40186-72-9	0.0006 (48)	8.1 (49)
Decachlorobiphenyl	PCB209	2051-24-3	0.0003 (48)	8.2 (49)
2,3,7,8-Tetrachlorodibenzodioxin	Dioxin	1746-01-6	0.0002 (50)	6.8 (51)

All analytes were reagent grade or better and used as received. Aniline and nitrobenzene were purchased from Sigma-Aldrich (St. Louis, MO). PCBs and dioxin were acquired from AccuStandard (New Haven, CT). Deuterated PCB compounds, which were used as surrogates

and internal standards during PCB analysis, were acquired from CDN Isotopes (Quebec, Canada).

Uptake and ENM-Water Equilibrium Partition Coefficient Experiments

ENM-water partition coefficients were obtained from the ratio between the concentration of the analyte sorbed on (or in) the ENM and the corresponding aqueous phase concentration of the analyte, with both concentrations measured at the same point in time (i.e., C_m/C_w). The initial aqueous concentration of aniline and nitrobenzene used in experiments was 25 μM ($\sim 2.8 \text{ mg/L}$). Amber glass vials (40 mL nominal volume) sealed with Teflon-lined screw caps were used in reactor assembly. The vials were filled completely with solution (i.e., there was no headspace) and $\sim 0.05 \text{ g}$ of ENM was added. Notably, uptake experiments were conducted with swatches of ENMs, roughly 3 cm by 8 cm in dimension. After assembly, the vials were placed on a rotator and tumbled end-over-end for a set period of time, with samples collected for measurement of aqueous and sorbed concentrations after 10 h, 1, 2, 3 and 5 days of mixing. Upon completion of the experiments, a final water sample was collected and the ENM was recovered for subsequent extraction to quantify sorbed analyte mass (as described in detail below). This allowed ENM-water partition coefficients to be calculated as a function of time in these reactors. These experimental steps employed to measure ENM-water partition coefficients are summarized in **Figure 8**.

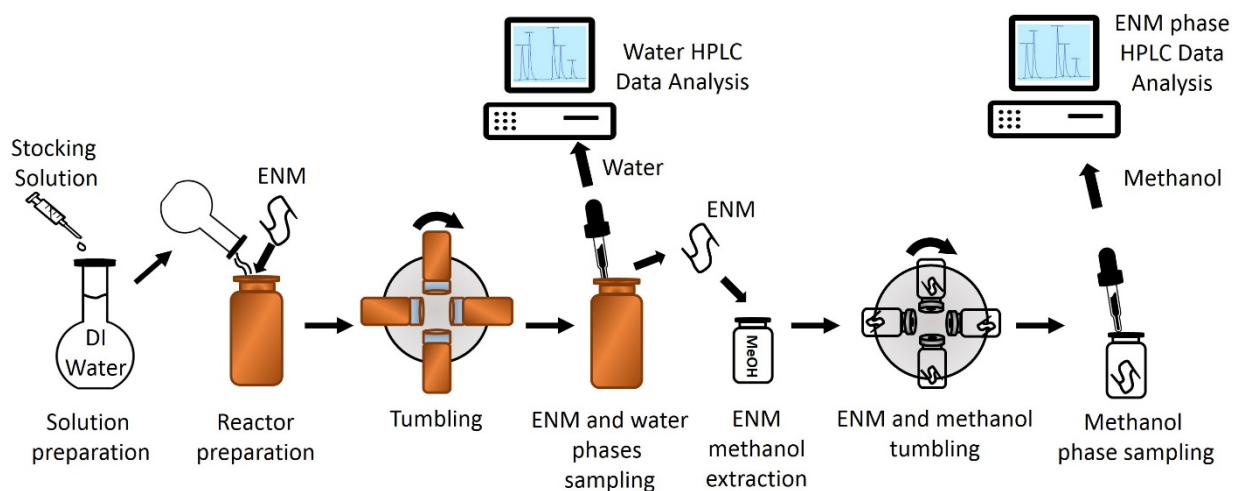


Figure 8. Flow diagram of the uptake and partition coefficient experiments for aniline and nitrobenzene.

For PCBs and dioxin, a similar approach was employed. Stock solutions of PCBs (0.1 to 100 ng/L) and dioxin (10 ng/L) were spiked into 40 mL amber glass vials sealed with Teflon-lined screw caps. No headspace was available, and $\sim 0.05 \text{ g}$ of ENM was added as the active sorbent. The glass vials were then placed on a rotator and tumbled end over end, with samples collected after 3, 5, 8 h and 1 d. Upon completion of the experiments, a final water sample was collected, and the ENM was recovered for subsequent extraction to quantify sorbed analyte mass. **Table 3** summarizes the matrix of analytes and polymer ENMs used in uptake experiments to quantify partition coefficients.

Table 3. Summary of the analytes and polymers for which ENM-water equilibrium partition coefficients were measured experimentally in homogeneous (water) systems.

ENM	Analytes			
	Aniline	Nitrobenzene	PCBs	Dioxin
PAN	✓	✓	✓	✓
PMMA	✓	✓	✓	✓
PS	✓	✓	✓	✓
PET	✓	✓	✓	✓
PVDF	✓	✓		
EVA	✓	✓		

For aniline and nitrobenzene, ENM-water partition coefficients were also measured across a range of pH values (from 5.5 to 9), where pH was controlled using commercially available buffers (MES, HEPES, AMPSO and BioXtra). In addition, sorption isotherm experiments were also conducted with aniline and nitrobenzene. These experiments followed a protocol similar to the aforementioned uptake experiments, but the initial aqueous concentration of aniline and nitrobenzene was varied from 10 to 200 μM (aniline: 1 - 19 mg/L, nitrobenzene: 1 – 25 mg/L) at a fixed ENM loading (0.05 g).

Finally, to explore the potential for simultaneous analysis of chemically diverse pollutant classes, uptake experiment were conducted in mixtures of aniline, nitrobenzene, PCBs and dioxins. These uptake experiments evaluated ENM-water partition coefficients over time, using the following analyte concentrations: aniline = 2.3 mg/L, nitrobenzene = 3 mg/L, PCBs1 and 11= 2500 ng/L, PCBs 29, 47, 121 and 136 = 250 ng/L, PCBs 187, 194, 206 and 209 = 125 ng/L, and dioxin = 250 ng/L. ENM-water partition coefficients from these mixture experiments could then be compared to values measured in experiments with individual analytes to determine if competitive inhibition of pollutant uptake occurred on ENMs.

Soil Preparation and Uptake Experiments

ENM uptake experiments were conducted in heterogeneous systems (i.e., water and soil) using a commercially available soil. A sandy loam (marketed as “LBLS” by AGVISE laboratories) with a soil organic carbon content of 3% (52) was used. For uptake experiments, the soil was first mixed with DI water (50% v/v). Then, the soil was sterilized with sodium azide (NaN_3), where 30 mM of sodium azide was mixed with the soil for 2 weeks. After sterilization, the soil system was then spiked with aniline or nitrobenzene to achieve an initial concentration of 100 μM (~11 mg/L of aniline and nitrobenzene). The soil was again tumbled for two additional weeks, after which 30 g of wet soil was combined with ~50 mg of ENM in a clean, amber glass vial. The soil was again tumbled for two additional weeks, after which 30 g of wet soil was combined with ~50 mg of ENM in a clean, amber glass vials. After ENM addition, vials were tumbled end over end, with samples collected after 5, 10, 15, 20 and 25 days.

For PCBs, sterilized soils were spiked with 1 mL of the commercially available stock solution from AccuStandard. This stock solution contained all 10 PCB congeners with concentrations ranging from 1 mg/L to 100 mg/L. For dioxin, our initial experiment revealed that toluene, the carrier solvent for dioxin in the commercial stock solution from AccuStandard, dissolved the PS-

ENM. Thus, it was not possible to perform heterogeneous water-soil system experiments for dioxin. We note that this challenge with dioxin ultimately limited the amount of data we could collect for PCBs, as initial experiments assessed PS-ENM performance toward a mixture of PCBs and dioxins. Thus, the dissolution of the PS-ENM by toluene also affected PCB data collection. Accordingly, we only had time to conduct one PCB experiment for the spiked soil-water system, and this experiment was only sampled once after 5 days.

At each sampling point, the ENM was removed, gently wiped with a paper towel to remove superficial residual soil, and rinsed with a small volume (~50 - 100 mL) of DI water. We note that to confirm removal of soil via this wiping and washing procedure, SEM images of cleaned ENMs were collected. After cleaning, ENMs were analyzed for sorbed aniline, nitrobenzene and PCBs concentration using the extraction procedures described below.

Table 4 summarizes the different type of ENMs and analytes used in these heterogeneous soil-water experimental systems.

Table 4. Summary table of the ENMs and analytes used in the spiked model soil experiments performed.

ENM/Analyte	Aniline	Nitrobenzene	PCBs
PS	✓	✓	✓
PMMA	✓	✓	✓
PS-PMMA-PS	✓	✓	
PS 30% CNT (COOH)	✓	✓	

Contaminated Sediment Measurements

In addition to model soils, uptake experiments were conducted with contaminated sediment from Indiana Harbor and Ship Canal (IHSC) located in East Chicago, Indiana. Through ongoing work at the University of Iowa (UI), these sediments have previously been analyzed for PCBs (both bulk and pore water concentrations) and had their geochemical properties characterized (4, 53). The protocol for these experiments was analogous to the aforementioned protocols with model soil systems, although soils were not sterilized with sodium azide prior to ENM addition. For these experiments, around 20 grams of sediment was mixed with DI water (50% v/v), and then an ENM, either PS or PMMA, was added to the vial. Samples of the ENM were then collected over time to analyze the bound analyte mass.

Due to time constraints, we were unable to perform equilibrium uptake experiments for ENMs in these sediments. Instead, we chose to measure the sediment pore water concentration over a timeframe (50 days) that should be sufficient for hydrophobic compounds like PCBs to achieve equilibrium.

Analytical Methods

During uptake experiments with ENMs, analyte concentrations were not only measured in water (i.e., the aqueous phase), but the amount bound to the ENM (i.e., the sorbed phase) was also simultaneously quantified. Details of these analytical methods are as follows:

Aniline and Nitrobenzene

For measurement of aqueous phase concentration, a 1 mL aliquot of the reactor aqueous phase was transferred to an amber autosampler vial. Sample aliquots were then immediately analyzed via high performance liquid chromatography with diode array detector (LC/DAD; Agilent 1100 Series HPLC). This system and associated analytic methods are described elsewhere (54, 55).

For measurement of the ENM-bound mass, both aniline and nitrobenzene were extracted from the ENM using methanol. Briefly, the ENM was added to a test tube with 10 mL of methanol and the mixture was subsequently tumbled for 2 days. Independent analysis found recovery (i.e., the extraction efficiency of this method) to be between 60 to 100% for aniline and nitrobenzene, respectively. After extraction, 1 mL of the methanol was transferred to an amber autosampler vial and analyzed for the concentration of dissolved aniline and nitrobenzene using LC/DAD. During LC/DAD analysis, we note that DI water and methanol blanks were analyzed with samples.

PCBs and Dioxin

PCBs and dioxin were measured using methods previously developed at the University of Iowa and reported elsewhere (44, 45), where analysis of PCBs and dioxins in the aqueous and ENM phases required extraction with hexane.

For aqueous phase analysis, 20 mL of aqueous sample was spiked with 25 ng of a PCB solution (PCB14, PCB65-d and PCB166) as a surrogate standard. The surrogate congeners were used to estimate any losses during the cleanup and extraction procedures. The mixture was then vortexed for 1 minute and subsequently mixed with 8 mL of hexane. This solution was tumbled for an additional 5 minutes, after which the hexane layer was separated from the water. The extracted hexane was concentrated using a Turbo Vap unit to around 0.5 mL and transferred to a gas chromatography (GC) vial. An internal standard consisting of 50 ng of PCB30-d and PCB204 was then spiked into this concentrated solution. PCBs and dioxin were then measured using gas chromatography with tandem mass spectrometry (GC-MS/MS, Agilent 7000) in multiple reaction monitoring mode (44, 53).

For analysis of the sorbed phase, the ENM was first spiked with 25 ng of a PCB surrogate standard and then tumbled with 40 mL of hexane for 12 h. The hexane was recovered via pipette and concentrated using a Turbo Vap unit to approximately 1 mL. An internal standard consisting of 50 ng of PCB30-d and PCB204 was then spiked into this concentrated solution. Samples were subsequently analyzed via GC-MS/MS, as described above for aqueous phase analysis.

Quality Assurance and Control (QA/QC)

Aniline and Nitrobenzene

Laboratory blanks consisted of DI water, methanol and unused ENMs. These blanks were extracted and analyzed in parallel with experimental samples (n=5). No contamination of aniline or nitrobenzene was found in any of the blanks analyzed. Further, a mass balance approach was carried out to calculate recoveries of aniline and nitrobenzene. Recovery of aniline through all the experiments ranged from 50% to 100%, whereas nitrobenzene recovery ranged from 80% to 100%. In the case of replicated measurements of aniline using PAN, PS and PMMA in homogeneous aqueous systems, a relative standard deviation (RSD) of 7% was obtained from 14

total measurements. Nitrobenzene yielded a RSD of 3%, also from 14 measurements. For the spiked soil experiments, a RSD of 24% and 14% for aniline and nitrobenzene, respectively, from 5 measurements were obtained. These RSD values are small and suggest excellent reproducibility throughout the entire experimental process.

PCBs and Dioxin

Laboratory blanks consisted of DI water, hexane and unused ENMs. These blanks were extracted and analyzed in parallel with experimental samples. No contamination of either PCBs or dioxin was observed in any of the blank media. Again, a mass balance approach was carried out to calculate recoveries of PCBs and dioxin. PCBs and dioxin mass recoveries ranged from 50% to 110%. Because we used an internal standard method to quantify PCBs and dioxin, we also determined the recoveries of the surrogate standards that were spiked into our samples prior to sample extraction and cleanup. For these compounds, the recoveries of PCB14, PCB-d65 and PCB166 averaged $87 \pm 7\%$, $85 \pm 9\%$ and $88 \pm 6\%$, respectively. In the case of replicated measurements of PCBs using PAN, PS and PMMA in homogeneous aqueous systems, a relative standard deviation (RSD) of 16% was obtained from 84 measurements (six PCB congeners). Dioxin yielded also a RSD of 16%, also from 12 measurements. These RSD values are very small and once again suggest excellent reproducibility throughout the entire experimental process.

Results and Discussions

Synthesis of ENMs via Electrospinning

ENMs of polyacrylonitrile (PAN), polystyrene (PS), polymethylmethacrylate (PMMA), polyvinyl acetate (PAVc), polyethylene terephthalate (PET), polyvinylidene fluoride (PVDF), and ethylene-vinyl acetate (EVA) were successfully fabricated using electrospinning. **Figure 9** shows images, both macroscopic and from SEM, of the seven ENMs produced in our laboratory. As shown in **Figure 9**, all ENMs consist of well-defined nanofibers, with the lone exception of EVA. We suspect the high viscoelasticity of the EVA polymer caused it to aggregate spontaneously after electrospinning. Thus, the average diameter of EVA-ENM fibers remained at the micron scale, forming more of a mesh rather than the non-woven nanofiber network observed for the other ENMs.

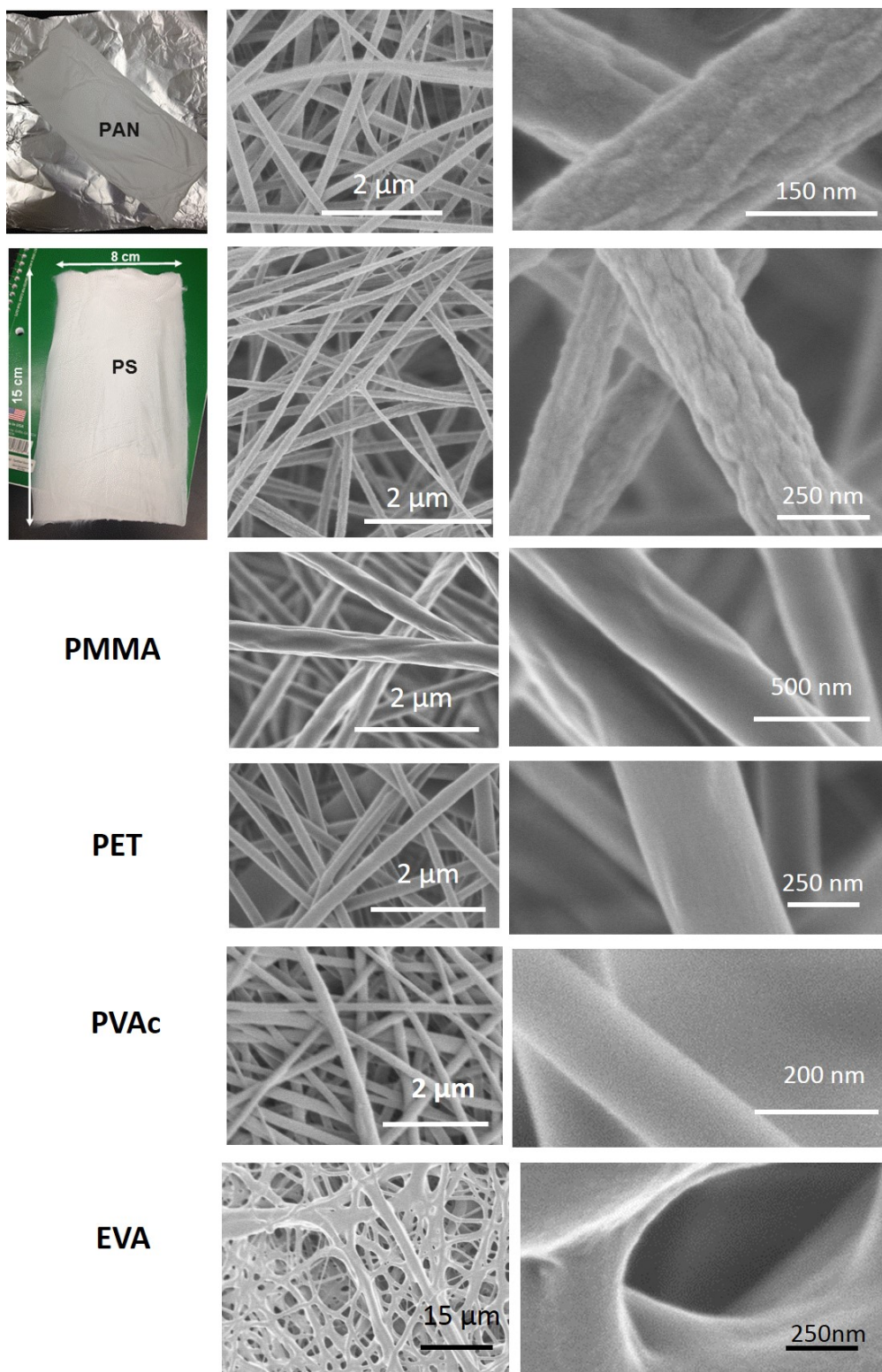


Figure 9. Images of polymer ENMs fabricated herein. ENM recipes are shown in Table 1.

Characterization of ENMs Surface Area, Nanofiber Diameter and Thickness

Generally, ENMs exhibited modest specific surface areas as analyzed by N₂-BET adsorption, and typically were of the range 5-30 m²/g. ENMs size distributions were quantified via SEM. Average diameters (with standard deviation) produced via our standard ENM recipes (see **Table 1**) are summarized in **Table 5**.

Table 5. Average diameters (with standard deviation) of nanofibers in standard ENM recipes (Table 1). Fiber diameters were measured from SEM images using ImageJ software. Typically, 100 nanofiber diameters were measured per ENM sample, allowing size distributions to be calculated for all synthesized materials. n = number of replicate syntheses.

	PAN	PS	PMMA	PVAc	PET	EVA
Average diameter (nm)	160 ± 30 (n = 7)	140 ± 30 (n = 4)	340 ± 50 (n = 6)	180 ± 30 (n = 3)	70 ± 20 (n = 4)	> 1000 (n = 2)

Distributions of nanofiber diameters were also used to assess the reproducibility of all ENM fabrication procedures. For example, **Figure 10** compares the nanofiber diameter distributions (shown as histograms) for four batches of PS-ENMs. These four batches were synthesized over the duration of the one-year SEED project, showing good batch-to-batch reproducibility in our fabrication protocols.

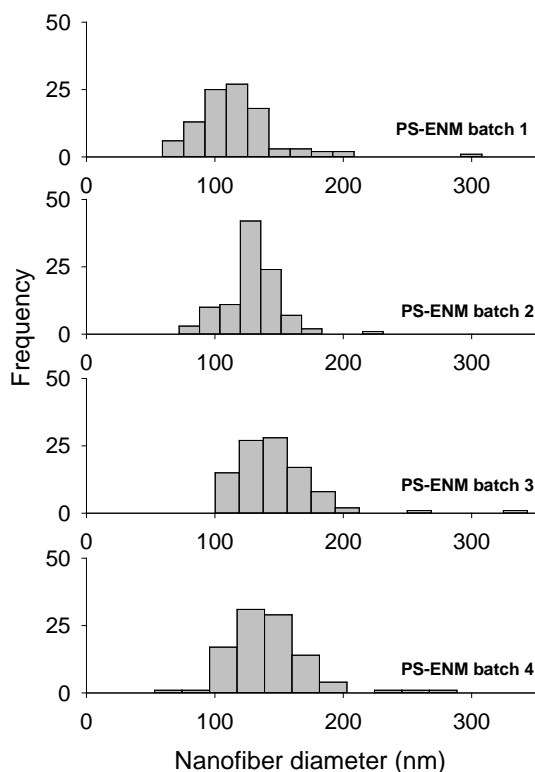


Figure 10. Histograms of four batches of PS-ENM fabricated over one-year SEED project. Diameters for at least 100 individual nanofibers within ENMs were quantified via SEM to produce these distributions.

Diameter size distributions also clearly demonstrate the impact of different synthesis variables on tunable ENM properties. For example, with PS, changes in relative humidity (from 5 to 50%) could be used to fabricate ENMs across a range of nanofiber diameters (**Figure 11**).

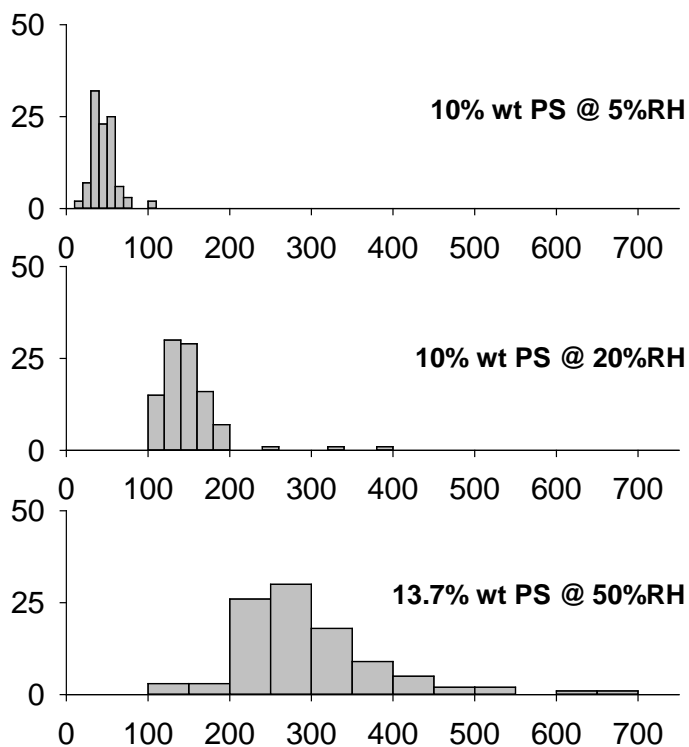


Figure 11. Histograms of three batches of PS-ENM fabricated as a function of relative humidity. Relative humidity could be used to tailor average diameter, with size distributions decreasing with decreasing relative humidity. Diameters for at least 100 individual nanofibers within ENMs were quantified via SEM to produce these distributions.

Similar results for the influence of humidity were also observed with other polymer nanofibers [e.g., the average diameter of PAN nanofibers increased from 100 (± 20) nm to 170 (± 30) nm from 5 to 20% RH]. Similarly, reducing the concentration of the polymer in the sol-gel and increasing the voltage during electrospinning resulted in a decrease in PS-ENM's nanofiber diameter (data not shown). In both cases, the decrease in nanofiber diameters result in an increase in the specific surface area (i.e., surface area per unit mass) of the ENM.

Finally, the thickness of ENMs was controlled by the volume of sol gel used during electrospinning. This is illustrated in **Figure 12** for PAN and PAN with integrated TBAB, which shows ENM thickness (as measured by cross sectional SEM imaging) as a function of sol gel volume. Depending on whether 2 to 6 mL of sol gel precursor was used during electrospinning, PAN mats exhibited thickness ranging from ~50 to 150 μm . As a result of the charge imparted by the cationic surfactant TBAB, the TBAB-containing mats were always thicker than their non-functionalized analogs. Thus, electrospinning affords outstanding control of ENM thickness, tunable entirely by the volume (or mass) of polymer used during synthesis.

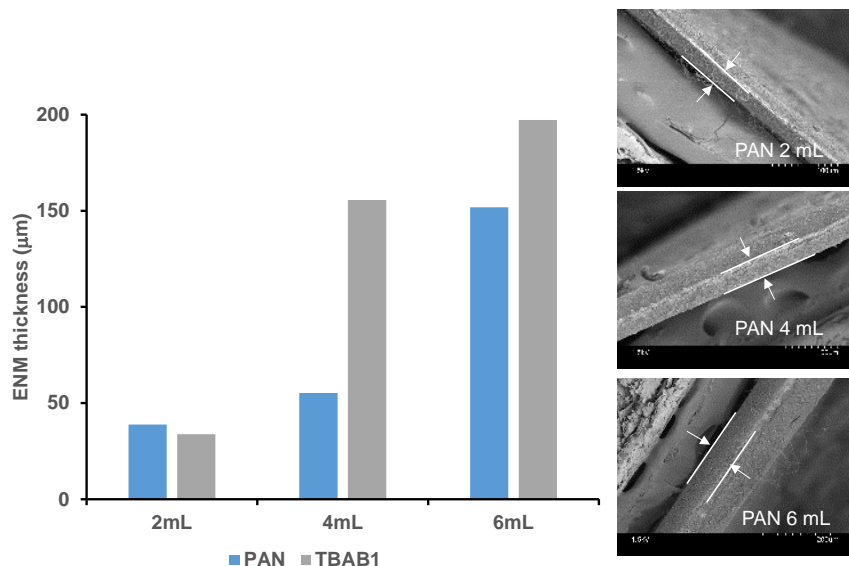


Figure 12. Influence of sol gel volume on the thickness (in μm) of PAN and PAN+TBAB ENMs. ENM thickness was quantified from cross-sectional SEM, with representative images shown.

Mechanical Testing and Chemical Stability of ENMs

Generally, all polymer ENMs were robust and durable. This is depicted in **Figure 13**, which shows images of a standard PS-ENM. Polymer ENMs were robust, able to support a reasonable load, and could be twisted and stretched without significant deformation.

ENMs were inert in most solvents. We tested ENM stability in solutions of pure acetone, dichloromethane, hexane, methanol and water, to simulate the range of solvents typically encountered during application or sample processing (e.g., extraction). No signs of polymer degradation or dissolution were observed for any of the solvents tested, with the exception of PVAc, which dissolved readily in methanol. Because methanol is commonly relied upon as an extraction solvent in passive sampler analysis, this observation of instability was used as grounds to no longer pursue PVAc-ENMs as viable passive sampling materials.

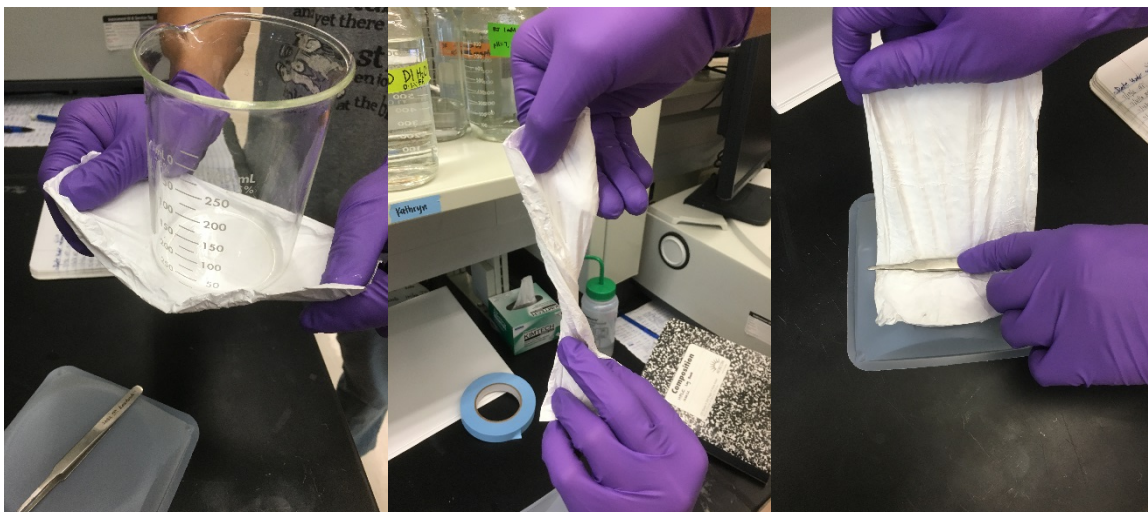


Figure 13. Photographs illustrating the handling, manipulation and mechanical strength of a representative PS-ENM.

Chemical Modification of ENMs and ENM Composites

Several chemically modified ENMs were synthesized via integration of select reagents (e.g., carbon nanotubes, surfactants) into polymer sol-gel solutions used for electrospinning. Generally, we found that ENMs produced with these modifications were comparable in character to their non-modified components. For example, while the integration of either non-functionalized or oxidized CNTs into PS changed the ENMs appearance (from white without CNTs to dark black with CNTs; **Figure 14**), PS-ENM with or without CNTs exhibited comparable average diameters (e.g., 140 ± 30 nm for PS versus 140 ± 40 nm for PS+CNT). Similarly, inclusion of surfactants (e.g., TBAB) into polymers also had little influence on nanofiber size distribution (**Figure 15**). *These characterization results for modified ENMs are important, as their physical similarity to unmodified analogs allows any difference in performance to be linked directly to chemical properties imparted via ENM modification.*

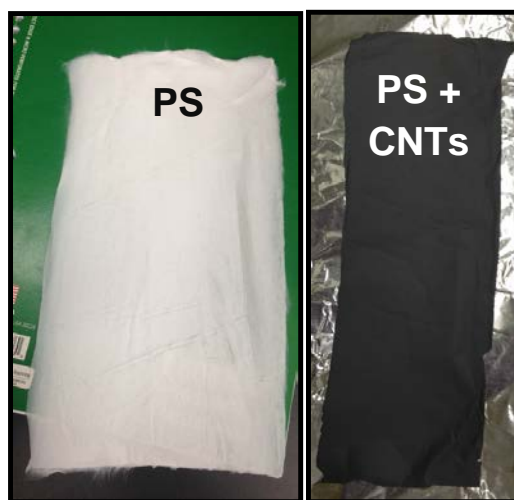


Figure 14. Picture of bulk PS-ENM (left) and a PS-ENM composite after integration of carbon nanotubes (CNTs) (right).

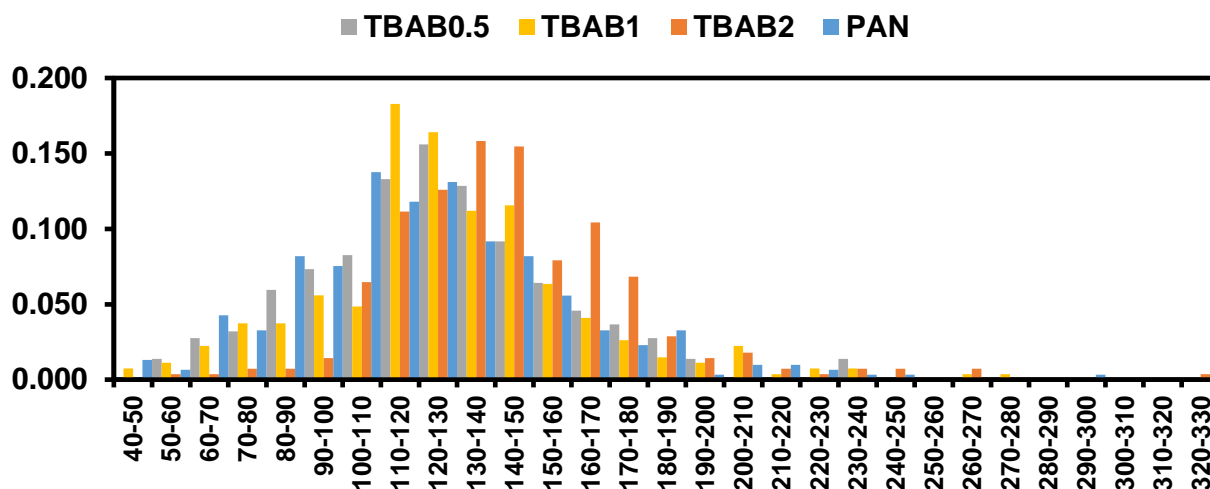


Figure 15. Diameter size distributions for PAN and PAN amended with three different loadings of the cationic surfactant TBAB (0.5, 1 and 2% by weight). Mean diameters (with standard deviation) are: 120 ± 40 nm for PAN; 130 ± 30 nm for TBAB0.5; 130 ± 40 nm for TBAB1; and 130 ± 30 nm for TBAB2.

Fabrication of Multilayer ENMs

We successfully fabricated several multilayer ENMs using sequential, layer-by-layer electrospinning of different polymers. Multilayer ENMs fabricated include PAN-PS, PAN-EVA, PS-EVA, and PS-PMMA-PS. Multilayer mats were cohesive, with layers firmly bound to one another. Thus, while possessing distinct layers of each polymer, the multilayer units functioned as a single ENM with spatially resolved polymer composition as a function of thickness.

Determination of Uptake Kinetics and ENM-Water Equilibrium Partition Coefficients

Polar Analytes: Aniline and Nitrobenzene

PAN, PMMA, PS and PET ENMs exhibited very fast equilibrium uptake (< 1 d) for both polar analytes (Figure 16). The average ENM-water partition coefficients for aniline and nitrobenzene are summarized in Table 6.

Table 6. Summary of ENM-water equilibrium partition coefficients [average and standard deviation as $\log(C_m/C_w)$ in L/kg] for aniline and nitrobenzene (NM = not measured).

Analyte	ENM Type					
	PAN	PMMA	PS	PET	PVDF	EVA
Aniline	1.9 ± 0.06 (n = 10)	1.7 ± 0.1 (n = 9)	1.5 ± 0.03 (n = 10)	1.4 ± 0.04 (n = 4)	0.72 ± 0.03 (n = 4)	NM
Nitrobenzene	1.9 ± 0.1 (n = 9)	2.8 ± 0.2 (n = 10)	2.8 ± 0.01 (n = 10)	2.2 ± 0.03 (n = 4)	NM	2 ± 0.01 (n = 4)

For aniline ($pK_a = 4.87$), a small ($\sim 1\%$) fraction of which is partially charged at the pH (pH 6.5) used in these experiments, partition coefficients were larger for more hydrophilic ENMs than for

hydrophobic ENMs (PAN > PMMA > PS > PET >> PVDF). For example, we found a significant difference in uptake between PAN and PVDF (Kruskal-Wallis one way ANOVA, $p < 0.001$), and PAN and PET ($p = 0.36$) for aniline. *Results with aniline, therefore, support one of the overriding hypothesis of our original SEED proposal. Specifically, hydrophilic ENMs exhibit greater uptake rates and capacities for polar (and even partially charged) analytes (e.g., aniline) relative to more hydrophobic ENMs.* This presumably is the result of favorable binding interactions associated with oxygen- and nitrogen- containing functional groups in hydrophilic polymers.

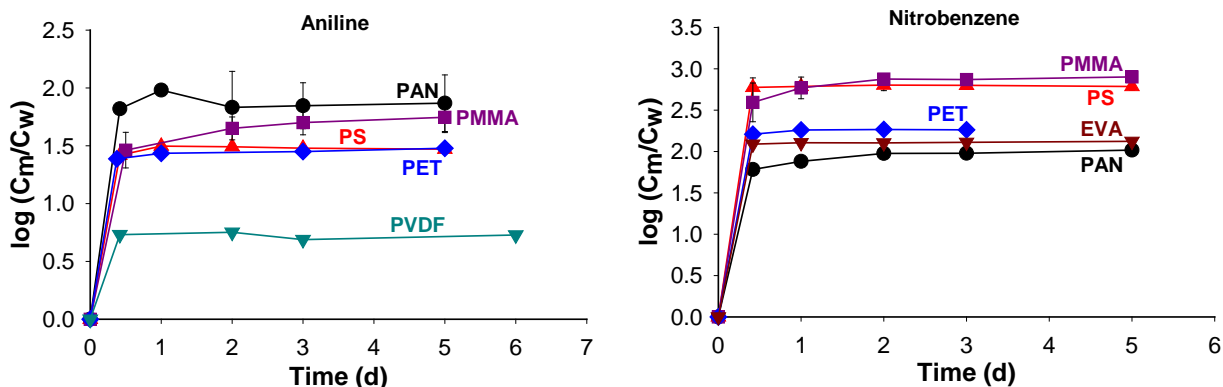


Figure 16. ENM uptake curves for aniline (left panel) and nitrobenzene (right panel) for our different ENMs. The error bars represent the standard deviation from two different uptake experiments. Laboratory set up: pH ~ 6.5 (DI water), initial aniline and nitrobenzene concentrations 25 μ M (aniline: 2 mg/L, nitrobenzene: 3 mg/L), ENM loading ~1.5 g/L. PAN-ENM, PS-ENM and PMMA-ENM). PAN, PMMA are hydrophilic ENMs; PET, PS and PVDF are hydrophobic; and EVA has both chemical groups.

For nitrobenzene, on the other hand, there was no clear relationship between uptake and polymer chemical characteristics, with partition coefficients for NB following: PMMA ~ PS > PET ~ EVA ~ PAN. Notably, while uptake was greatest on PMMA (which we have classified as a polar/hydrophilic polymer), nearly comparable uptake was observed for hydrophobic PS-ENM. Likewise, the lowest degree of uptake was observed with PAN-ENM, a hydrophilic polymer. Unlike aniline (with an ionizable and electron donating $-\text{NH}_2$ group attached to the benzene ring), nitrobenzene is neutrally charged over the pH ranges we have considered and possesses a strongly electron withdrawing nitro ($-\text{NO}_2$) group. Thus, differences in the relative trends of ENM uptake between aniline and nitrobenzene likely reflect distinct physical and chemical binding interactions between each analyte and the polymeric ENMs. More work is needed to elucidate the factors driving nitrobenzene uptake, but we suspect that multiple factors (e.g., hydrophobic exclusion of the aromatic ring in combination with specific binding interaction via the nitro moiety) contribute simultaneously to NB partitioning into ENMs.

Using the results in **Figure 16**, and factoring in their relative ease of fabrication, an initial prioritization of the most promising ENMs for targeting polar analytes was conducted. For example, EVA was not considered a promising passive sampling material as a result of

difficulties in electrospinning uniform nanofibers, along with its modest performance toward polar analytes, In contrast, due to their strong performance toward both aniline and nitrobenzene and relative ease of fabrication, polystyrene (PS) and polymethylmethacrylate (PMMA) were prioritized as promising materials for further optimization and testing. In addition, PAN was chosen for additional investigation, largely because of several recipes that we have developed for tailoring the chemical properties of PAN-ENMs.

Hydrophobic Analytes: PCBs and Dioxin

Using the ENMs prioritized as described above (PMMA, PAN and PS), additional experiments were conducted to explore their uptake of PCBs and dioxin. Because these are hydrophobic analytes, we elected to include another hydrophobic polymer, PET, for additional comparison.

Once again, all four ENMs exhibited very fast equilibration times (< 18 h) with both PCBs and dioxin (**Figure 17**). We note that preliminary uptake experiments revealed that PCBs 187, 196, 206 and 209 were not completely dissolved in the aqueous phase. Thus, these four congeners were not considered further in our ENM equilibrium partitioning experiments. The ENM-water partition coefficients for PCBs and these four ENMs are summarized in **Table 7**, with the corresponding time-dependent partition data provided in **Figure 17**. The partition coefficient values ranged from 2.4 to 6.3 (L/kg), depending on the chemical and the ENM used.

Table 7. Summary of ENM-water equilibrium partition coefficients [average and standard deviation as $\log(C_m/C_w)$ in L/kg] for selected PCB congeners and dioxin.

ENMs	PCB1	PCB11	PCB29	PCB47	PCB121	PCB136	Dioxin
PAN (n=2)	3.6 ± 0.1	4.3 ± 0.1	4.3 ± 0.1	4.3 ± 0.1	4.4 ± 0.2	4.4 ± 0.1	3.2 ± 0.1
PS (n=2)	4.8 ± 0.1	5.3 ± 0.1	5.1 ± 0.1	4.8 ± 0.1	5.1 ± 0.2	5.4 ± 0.2	5.3 ± 0.3
PMMA (n=2)	4.8 ± 0.1	5.2 ± 0.2	5.3 ± 0.1	4.8 ± 0.1	5.7 ± 0.1	6.0 ± 0.4	6.4 ± 0.1
PET (n=2)	3.9 ± 0.3	4.8 ± 0.2	4.8 ± 0.2	4.8 ± 0.1	5.1 ± 0.2	4.9 ± 0.2	4.5 ± 0.1

As with polar targets, PS and PMMA tended to produce the greatest equilibrium partition coefficients toward all hydrophobic analytes. Accordingly, PS and PMMA were once again prioritized as the most promising materials for further optimization and testing as passive sampling materials.

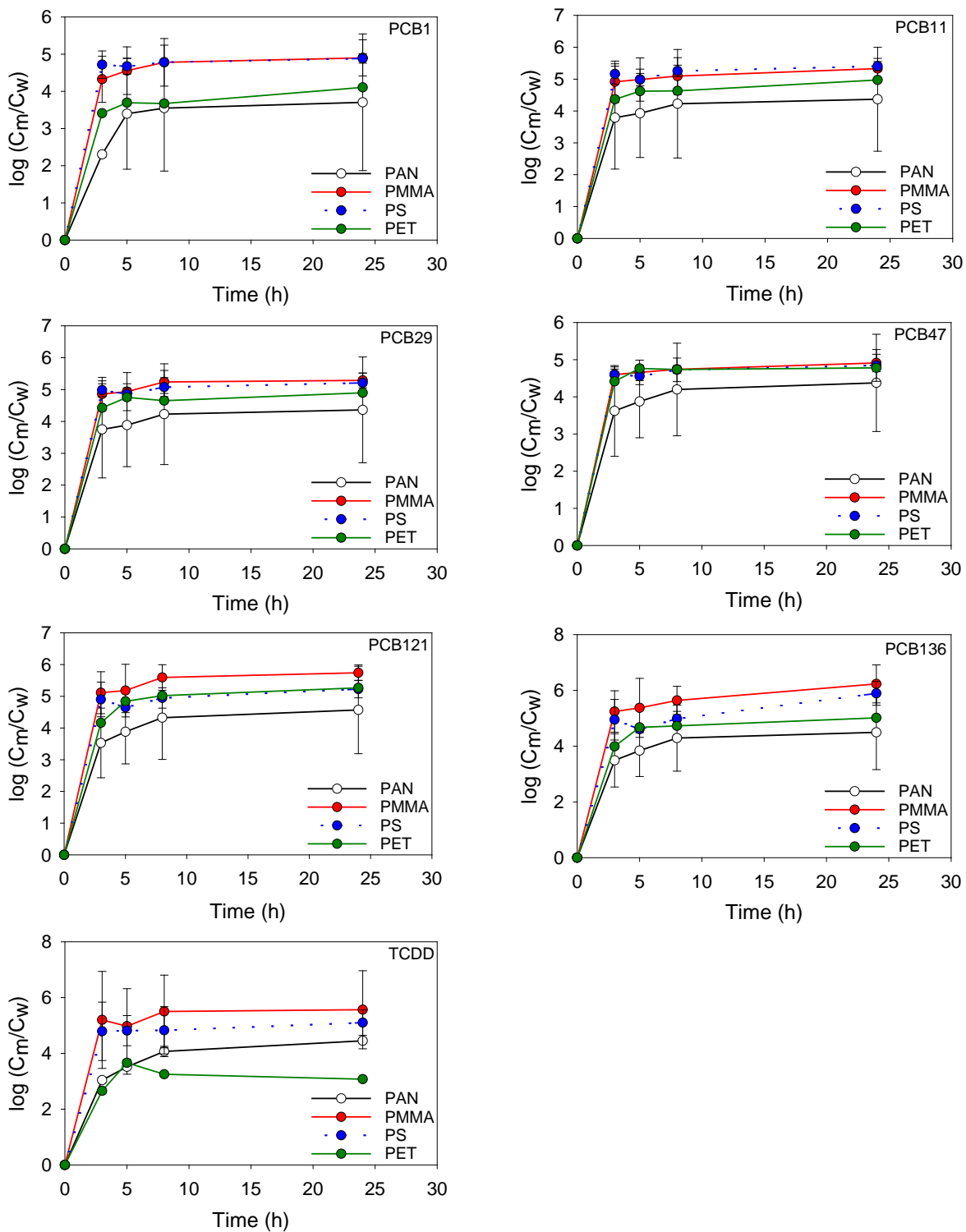


Figure 17. ENM uptake curves for selected PCB congeners and dioxin (TCDD). The error bars represent the standard deviation from two different uptake experiments. Laboratory set up: pH ~ 6.5 (DI water), initial concentrations from 0.25 to 5 ng/L, ENM loading ~3 g/L.

Influence of Solution Phase Variables on Performance of Prioritized ENMs.

Influence of pH on Aniline and Nitrobenzene Uptake

Solution pH can play a critical role in sorbent performance, particularly for charged analytes or for surface functional groups on the sorbent that may be ionizable across ambient pH ranges of surface waters and sediments. Here, we explored whether ENM-water equilibrium partition coefficients for aniline and nitrobenzene changed across a range of environmentally relevant pH values for PS-ENM and PMMA-ENM. Partition coefficients were measured over a range of environmentally relevant pH values (5.5 to 9) in buffered systems (i.e., the pH did not change over the duration of the uptake experiment).

As shown in **Figure 18**, we found that ENM-water partition coefficients were generally independent of pH for both polar analytes. While further work is merited, a slight pH dependence observed for aniline at low pH may reflect different modes of uptake on PMMA and PS. For example, hydrophilic PMMA exhibited more uptake at lower pH values, where a greater fraction of aniline mass is positively charged (roughly ~50% of total aniline mass is positively charged at pH 5.5). Meanwhile, aniline uptake is essentially independent across pH on PS, but notably lower than on PMMA. Thus, the greater net uptake of aniline on PMMA, as well as a slight pH-dependence in partition coefficients in more acidic regimes, may reflect a favorable role for electrostatic or specific binding interactions in uptake. In contrast, uptake of aniline on PS may be limited to only hydrophobic exclusion (presumably localized to the aromatic ring of aniline), the driving force for which would be independent of pH.

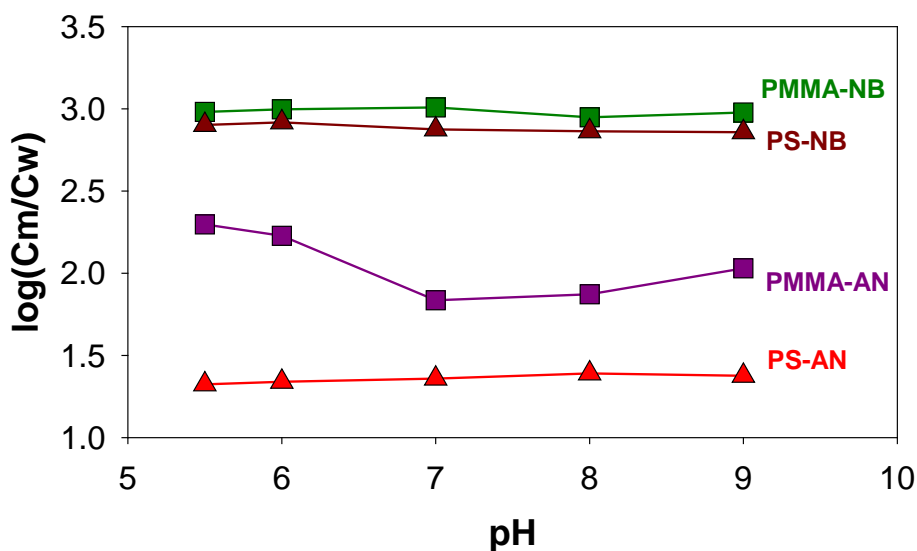


Figure 18. ENM-water equilibrium partition coefficients (L/kg) for aniline (AN) and nitrobenzene (NB) measured as a function of solution pH for PS-ENM and PMMA-ENM. Laboratory set up: initial aniline and nitrobenzene concentrations 25 μ M (aniline: 2 mg/L, nitrobenzene: 3 mg/L), ENM loading ~1.5 g/L. Experiments were performed for 5 days. pH was controlled using commercially available buffers (MES, HEPES, AMPSO and BioXtra).

Influence of Aniline and Nitrobenzene Concentration on ENM-Water Partitioning

Additional experiments assessed ENM performance across a range of analyte concentrations (at a fixed ENM mass loading), which is relevant to the potential use of ENMs at sites where pollutant levels may vary spatially or temporally. These isotherm experiments were conducted at pH 7 with PMMA-ENM and PS-ENM with both polar analytes from 10-200 μM (Aniline 1.0 - 20 mg/L, nitrobenzene 1.0 - 25 mg/L).

In general, linear sorption isotherms were obtained for aniline and nitrobenzene on both PS-ENM and PMMA-ENM (**Figure 19**). However, aniline exhibited deviation from linearity at the highest aqueous concentration explored (200 μM or 20 mg/L), indicative of sorbent saturation under such conditions. Accordingly, this point was not included in the linear regression analysis shown in **Figure 19**. Via this linear regression analysis, ENM-water equilibrium partition coefficients could be calculated from the linear isotherm slope (C_m/C_w , L/kg). This resulted in very similar values to those obtained from the aforementioned time-dependent partition coefficient experiments (see **Table 6**).

Isotherm results indicate that at the concentration levels explored herein ($< \sim 150 \mu\text{M}$ or $\sim 15 \text{ mg/L}$), the ENM-water equilibrium partition coefficients are independent of the aqueous concentration. These results are consistent with aniline and nitrobenzene uptake on both ENMs being primarily an absorption (bulk uptake) process. Notably, the concentrations used herein far exceed those likely to be encountered at contaminated sites. Thus, field deployment of ENMs should result in partitioning that scales in a linear fashion with the dissolved concentration of polar analytes in surface or sediment pore water.

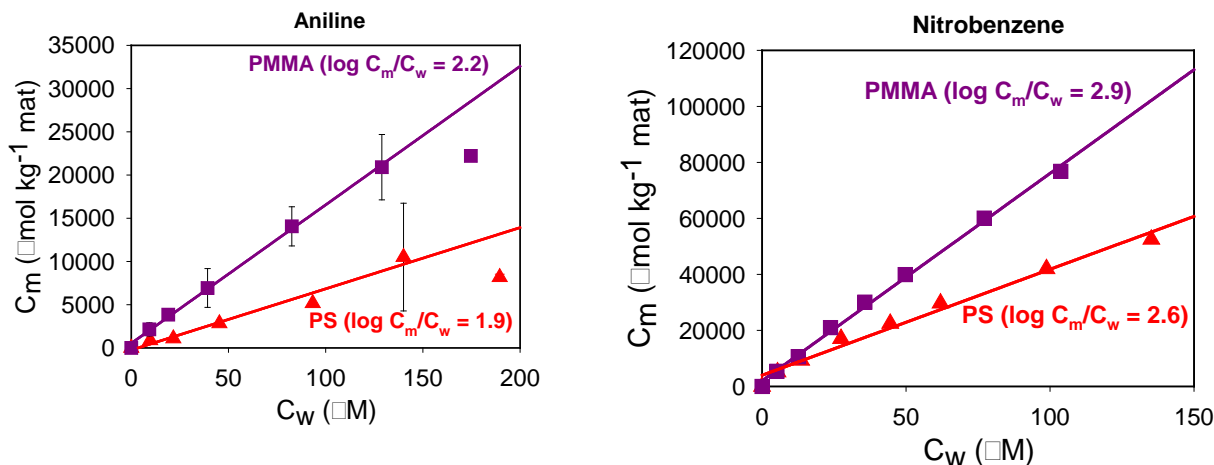


Figure 19. Sorption isotherms using PS-ENM and PMMA-ENM for aniline (left panel) and nitrobenzene (right panel). Initial aqueous concentrations varied from 10 to 200 μM (aniline: 1 - 19 mg/L, nitrobenzene: 1 - 25 mg/L). The error bars represent the standard deviation from two different uptake experiments. Laboratory set up: pH ~ 6.5 (DI water), and ENM loading $\sim 1.5 \text{ g/L}$. Experiments were performed for 5 days.

ENM Performance in Multi-Target Pollutant Mixtures.

Solutions with mixtures of all target analytes (i.e., aniline, nitrobenzene, PCBs and dioxin) were prepared, and partition coefficients for each target were measured in the presence of the other, potential competitors for ENM uptake. Notably, on PS and PMMA, partition coefficients measured in these mixtures were identical to those measured with each target in isolation. *Thus, experimental evidence suggests that ENMs are capable of simultaneous and non-competitive uptake of diverse pollutant classes across a range of $\log K_{ow}$ values. This outcome supports our original vision for an ENM-based passive sampler suitable for multi-target analysis.*

Further Optimization of Promising ENMs to Improve Sampler Performance

All results thus far have highlighted the promise of PS- and PMMA-ENMs for the uptake of both hydrophilic and hydrophobic analytes in homogeneous aqueous systems. As noted earlier, PAN-ENMs are another intriguing option. While their measured partition coefficients may not always be as large as those of PS- and PMMA-ENMs, there are several established electrospinning recipes (in the literature and developed in our labs) that allow for the facile tuning of PAN-ENM properties.

Here, we summarize results of several attempts to further improve the performance of ENMs through tailored synthesis and integration of chemically active components. These experiments focused exclusively on PS-ENMs and PAN-ENMs. Although PMMA-ENM yielded relatively high partition coefficients for target analytes, its electrospinning sol-gel solution uses glacial acetic acid to increase conductivity during electrospinning. Unfortunately, preliminary experiments revealed this acid to more readily destabilize sol-gels with other component materials added, thereby complicating synthesis of modified PMMA-ENMs.

Influence of ENM Average Diameter on Polar Analyte Uptake

We initially hypothesized that smaller nanofiber diameters (and therefore higher ENM specific surface area in m^2/g) would increase the rate and extent of analyte partitioning into ENMs. However, uptake studies with two different PS samples showed that nanofiber diameter exerted little influence on ENM-water partition coefficients. Experiments were conducted with PS-ENMs with mean diameters of 45 (± 15) nm and 150 (± 40) nm, yielding ENM-water partition coefficients of 1.48 and 1.41, respectively, for aniline and 2.6 and 2.5, respectively, for nitrobenzene. *The invariance of these partition coefficients across PS-ENM diameter suggests that ENM mass rather than surface area is the dominant factor controlling uptake. This is consistent with a mechanism of polar analyte uptake where partitioning into the bulk of the nanofibers comprising the ENM is the dominant mechanism for uptake (i.e., absorption) rather than simple binding on the ENM nanofiber surface (i.e., adsorption) (56, 57).*

Influence of CNT Integration on Polar Analyte Uptake.

CNTs are often integrated into polymer nanofibers to increase their strength. Further, we have recently found that integration of CNTs into ENMs can also influence the rate and extent of sorption of polar analytes (41). Here, two forms of CNTs, non-functionalized (or as-received) and carboxylated (with a majority of surface $-COOH$ sites), were integrated into PS-ENM. The non-functionalized CNTs are largely hydrophobic, whereas the carboxylated CNTs would possess a negative surface charge at the pH values considered in these experiments (i.e., the

majority of –COOH surface groups are deprotonated near pH 7) and thereby impart negative charge to the ENM surface.

Results from time-dependent uptake studies for aniline and nitrobenzene are shown in **Figure 20** for PS-ENMs amended with non-functionalized and carboxylated CNTs. The greatest effect was observed for aniline, where partition coefficients increased with increase loading of carboxylated CNTs. A much slighter increase in partition coefficients was observed for PS amended with non-functionalized CNTs. Accordingly, we believe the negative charge imparted by the carboxylated CNTs is responsible for the increased uptake of aniline, a small fraction of which (~ 1%) is positively charged at pH 7. The partition coefficients for ENMs amended with CNTs are summarized in **Table 8**. For aniline, all of these values are greater than those values measured with non-CNT containing PS-ENMs (see **Table 6**).

Table 8. Partition coefficients [average and standard deviation as $\log(C_m/C_w)$ in L/kg] for aniline and nitrobenzene using ENM integrated with CNTs (NM = not measured).

Analyte	ENM Type			
	PS 20% CNT	PS 30% CNT	PS 20% CNT (COOH)	PS 30% CNT (COOH)
Aniline	1.6 ± 0.2	1.7 ± 0.1	1.9 ± 0.1	2.1 ± 0.1
Nitrobenzene	NM	3.0 ± 0.03	2.9 ± 0.02	3.0 ± 0.04

Consistent with the surface charge of carboxylated CNTs being responsible for increased aniline uptake, integration of either type of CNT had little to no effect on nitrobenzene uptake. *Thus, in addition to increasing polymer ENM strength, incorporation of carboxylated CNTs is a promising way to promote uptake of polar species that exhibit partial positive charge in solution.*

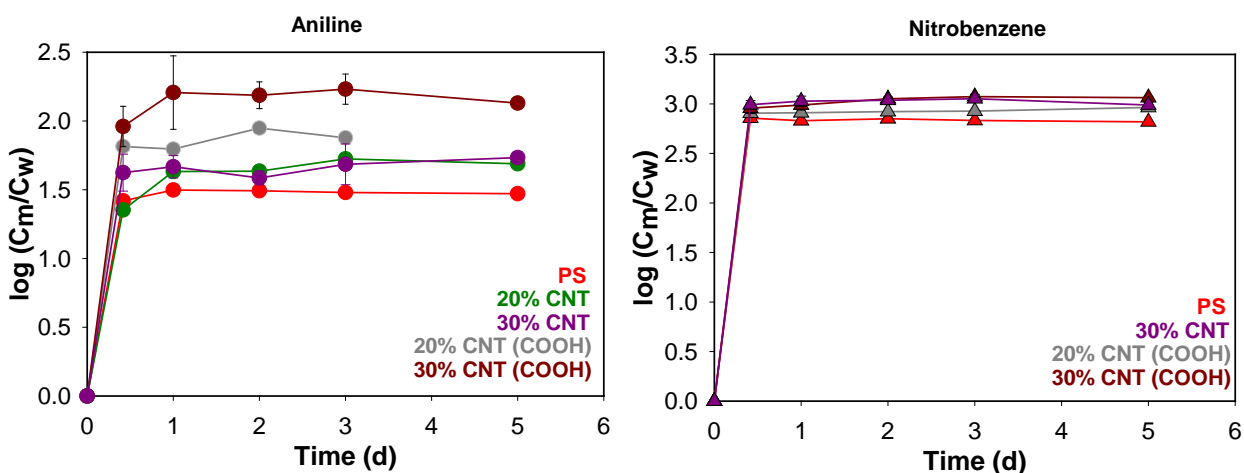


Figure 20. ENM uptake curves for aniline (left panel) and nitrobenzene (right panel) for modified CNT ENMs. The error bars represent the standard deviation from two different uptake experiments. Laboratory set up: pH ~ 6.5 (DI water), initial aniline and nitrobenzene concentrations 25 μ M (aniline: 2 mg/L, nitrobenzene: 3 mg/L), ENM loading ~1.5 g/L.

Influence of CNT Integration on Hydrophobic Analyte Uptake.

Uptake experiments for PCBs and dioxins were also carried out using PS-ENMs amended with non-functionalized and carboxylated CNTs. Partition coefficients for PCBs did not show any significant difference for the low chlorinated PCB congeners (PCBs 1 and 11) in comparison with PS-ENM without CNTs. However, the more chlorinated congeners (PCBs 29, 47, 121 and 136) showed an increase in the partition coefficient (typically by ~0.5 log units) for PS composites using non-functionalized CNTs (**Table 9**). These results are consistent with the hydrophobic nature of non-functionalized CNTs, and thus they would be expected to promote uptake of more hydrophobic targets. Dioxin exhibited a reduction in partition coefficient on PS-CNT composites, although the origins for this decrease in uptake are not yet fully understood.

Table 9. ENM-water equilibrium partition coefficients [as $\log(C_m/C_w)$ in L/kg] for selected PCB congeners and dioxin for PS-ENM amended with CNTs.

Analyte	ENM Type		
	PS 30% CNT	PS 30% CNT (COOH)	PS (from Table 7)
PCB1	4.8	4.6	4.8
PCB11	5.1	5.2	5.3
PCB29	5.8	5.2	5.1
PCB47	5.3	5.0	4.8
PCB121	5.9	5.2	5.1
PCB136	5.8	5.4	5.4
Dioxin	3.6	4.7	5.3

Influence of Cationic and Anionic Surfactant Integration on Polar Analyte Uptake.

Another potential way to alter the surface chemical properties of ENMs is via incorporation of cationic and anionic surfactants. Retention of charged surfactants in the ENM matrix will in turn alter the net charge of the material to reflect that of the surfactant.

Here, two forms of surfactant modified ENMs were tested. These included PAN integrated with either sodium dodecyl sulfonate (SDS), an anionic surfactant, or tetrabutylammonium bromide (TBAB), a cationic surfactant. **Figure 21** shows uptake of aniline and nitrobenzene on SDS and TBAB modified PAN-ENMs. Once again, the most notable results occurred with aniline, where integration of positively charged TBAB inhibited uptake relative to unamended PAN. In contrast, integration of the anionic surfactant SDS increased the ENM-water partition coefficient by roughly one log unit relative to unamended PAN. As with the negatively charged carboxylated CNTs, we believe this positive influence on aniline uptake results from favorable electrostatic interactions between the negatively charged ENM surface and aniline, a small fraction (~1%) of which is positively charged near pH 7. This also would be consistent with the decrease in partition coefficient observed with integration of positively charged TBAB, which would produce unfavorable (repulsive) electrostatic interactions between the positively charged surface and aniline. Finally, no significant influence of SDS or TBAB on nitrobenzene uptake was observed, also suggesting that integration of surfactants appears most promising for improving performance of ENMs toward polar analytes that carry partial charge (e.g., ionizable analytes).

Influence of Chemical Functionalization via Amidoximation on Polar Analyte Uptake.

A benefit of PAN-ENMs is that its nitrile group can be chemically transformed into an amidoxime functionality via reduction with hydroxyl amine. The amidoxime group, which contains both $-OH$ and $-NH_2$ moieties, represents a promising chelating agent for metals and other charged analytes (58).

Here, amidoximation resulted in poorer performance toward polar analytes relative to PAN-ENMs. For example, after amidoximation, the ENM-water partition coefficient decreased considerably (by ~ 1.6 log units). A smaller, but still negative, influence on nitrobenzene uptake was also observed (~ 0.25 log units). While amidoximation does not appear to be an effective functionalization route to promote aniline or nitrobenzene uptake, it may still be suitable for other polar analytes that are more susceptible to favorable binding interactions with the surface $-OH$ and $-NH_2$ groups imparted by amidoximation.

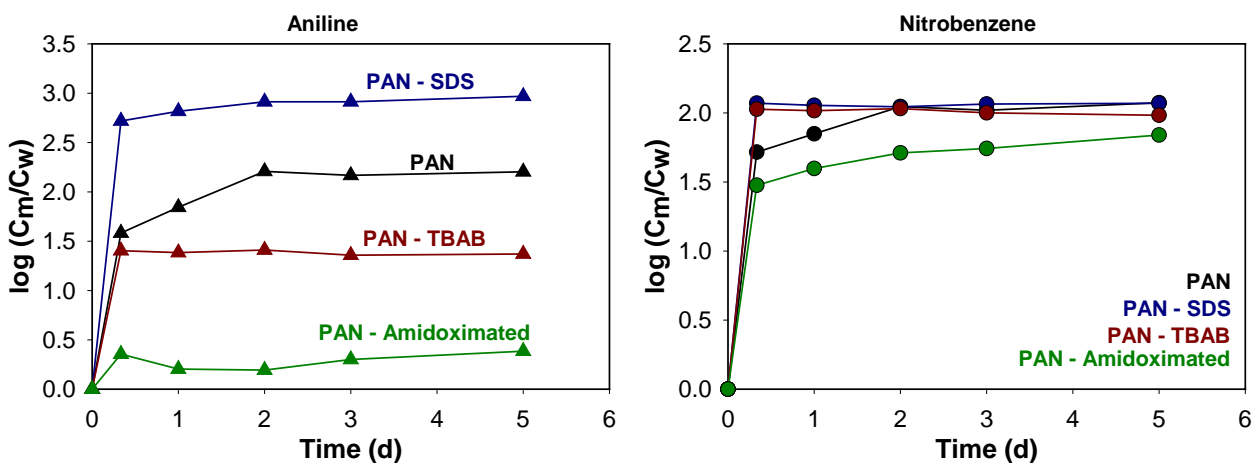


Figure 21. ENM uptake curves for aniline (left panel) and nitrobenzene (right panel) for surfactant and amidoximated modified PAN-ENMs. Laboratory set up: pH ~ 6.5 (DI water), initial aniline and nitrobenzene concentrations $25 \mu M$ (aniline: 2 mg/L , nitrobenzene: 3 mg/L), ENM loading $\sim 1.5 \text{ g/L}$.

Influence of Biocidal Agents on Polar Analyte Uptake.

A common concern during application of passive samplers is biofouling. Thus, agents that can be incorporated into the sampling material that impart biocidal activity without influencing target analyte uptake are desirable.

Here, we incorporated silver (Ag) nanoparticles into PAN-ENMs and PS-ENMs and assessed the influence of integrated Ag nanoparticles on aniline and nitrobenzene uptake. Silver nanoparticles are known to be biocidal, and have also been used to slow fouling on other surfaces including membranes used for water treatment (59). The integrated Ag nanoparticles had no effect on PS-ENMs performance toward both analytes, but did slightly decrease aniline and nitrobenzene uptake on PAN-ENMs (**Figure 22**). Nevertheless, the extent of uptake in all cases was still significant, such that integration of Ag as a biocide remains a promising option for fouling control in ENM application.

We note that another common antimicrobial agent is TBAB, which we have also used herein as a cationic surfactant to alter ENM surface charge. TBAB is a quaternary ammonium salt, a class of chemicals recognized for their biocidal activity (60). In fact, TBAB amended nanofibers have been developed in our laboratory for water treatment, where a single pass of solution through a TBAB-modified PAN-ENM can achieve up to 6-log removal of pathogenic viruses. Further, we have found that TBAB is stable within the PAN-ENM matrix during such applications (i.e., it does not wash out over time). As shown earlier, TBAB also has little to no impact on the uptake of neutral nitrobenzene. Thus, it may represent another promising route to impart biocidal activity to ENMs during their application as passive sampling devices in complex media (e.g., sediments).

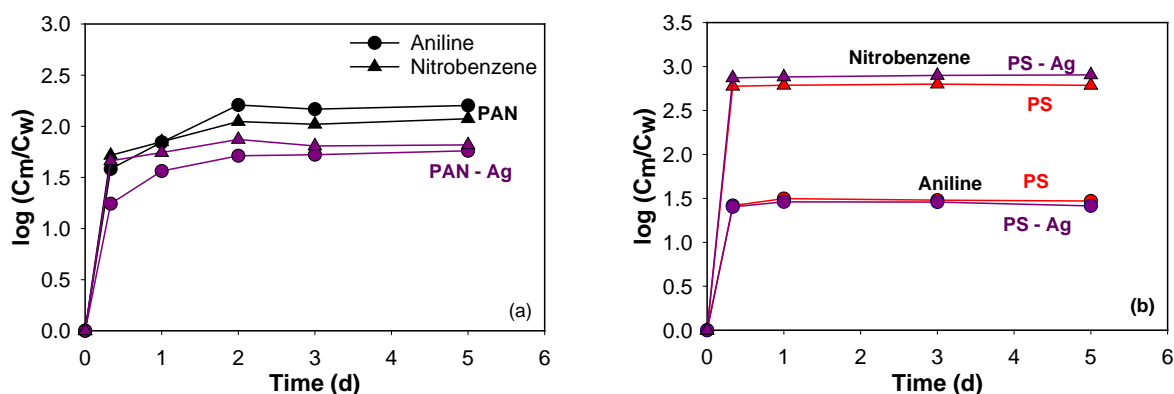


Figure 22. ENM uptake curves for aniline (circle) and nitrobenzene (triangle) for silver nanoparticle modified PAN (panel a) and PS (panel b) ENMs. Laboratory set up: pH ~ 6.5 (DI water), initial aniline and nitrobenzene concentrations 25 μ M (aniline: 2 mg/L, nitrobenzene: 3 mg/L), ENM loading ~1.5 g/L.

Performance of Multilayer ENMs.

Another benefit of ENMs is their ability to be fabricated layer-by-layer, allowing production of multilayer mats where each layer can possess unique physical and chemical properties. This allows another fabrication approach by which material performance for passive sampling can be improved, producing a multilayer structure with potential synergies in performance and opportunities for improved spatial data resolution relative to single layer ENMs.

Accordingly, several bi-layer and tri-layer ENM formulations were fabricated and tested for uptake of aniline and nitrobenzene. Generally, partition coefficients on multilayer materials were at best equivalent to the value measured with its most reactive component (as a single ENM layer), or at worst the average of the partition coefficients measured across its multiple ENM components. For example, bilayer PAN-PS-ENM yielded an ENM-water equilibrium partition coefficient of 1.7 log units for aniline, which falls in between to the partition coefficients measured for each individual components, PS-ENM (1.5) and PAN-ENM (2.1).

These results are promising. While it may be possible to identify a single polymer ENM with sufficient capacity for a chemically diverse set of pollutant targets, it may also be advantageous to fabricate multilayer ENMs where each layer is specifically designed to target a different pollutant class. Alternatively, it may also be possible to couple inert or antifouling outer layers with an active inner layer tuned for pollutant uptake, developing a “sandwich” packing that improves functionality of the overall unit by preventing bio- or organic matter fouling to the encapsulated active sorbent ENM.

Summary ENM Performance and Comparison to Commercially Available Materials.

Figure 23 and **Figure 24** summarize all ENM-water partition coefficients [as $\log(C_m/C_w)$ in L/kg] measured herein for aniline and nitrobenzene, respectively. The figures illustrate that ENM-water partition coefficients span almost 3-log units for aniline and 1.5-log units for nitrobenzene, depending on the type of polymer and chemical modification approaches used for ENM fabrication. These summary figures are valuable for identifying the ENMs with the greatest affinity for the polar analytes investigated herein (i.e., SDS modified PAN for aniline and most PS containing ENMs for nitrobenzene).

Another important feature of these figures is that we have included corresponding partition coefficients that we have measured for aniline and nitrobenzene using conventional, commercially available passive sampling materials. Experiments with these commercially available materials were conducted using the same conditions as for uptake studies with ENMs, and used an equivalent amount of sorbent mass. Commercial sorbent materials evaluated include polystyrene beads, a PDMS fiber (the composition of SPME fibers), and a low-density polyethylene (LDPE) film, many of which have been used in research and development of passive sampling materials, albeit mostly for hydrophobic compounds (4, 5, 44).

***Figure 23** and **Figure 24** clearly show the advantages of ENMs over current commercial options for passive sampling materials. For aniline, no uptake on LDPE was observed, while partition coefficients for PS beads and PDMS fibers were nearly 2-log units smaller than measured for the most reactive ENM that we produced. Surprisingly, uptake of nitrobenzene was not measurable over our standard experimental timescale for any of the commercial materials, further highlighting the dearth of passive sampling materials currently available for polar analytes.*

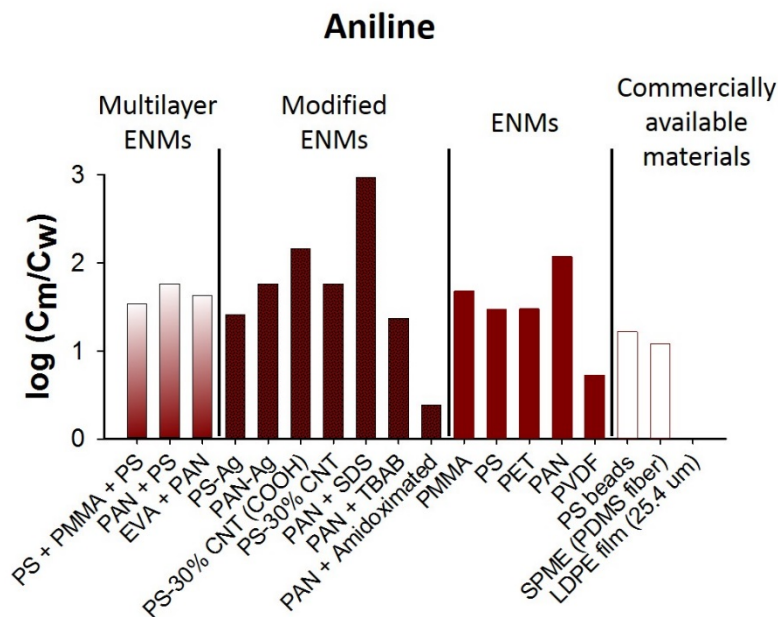


Figure 23. Summary of the ENM-water equilibrium partition coefficients for aniline obtained for all of the ENMs synthesized. Commercially available materials were also included such as PS beads, PDMS fiber and LDPE film.

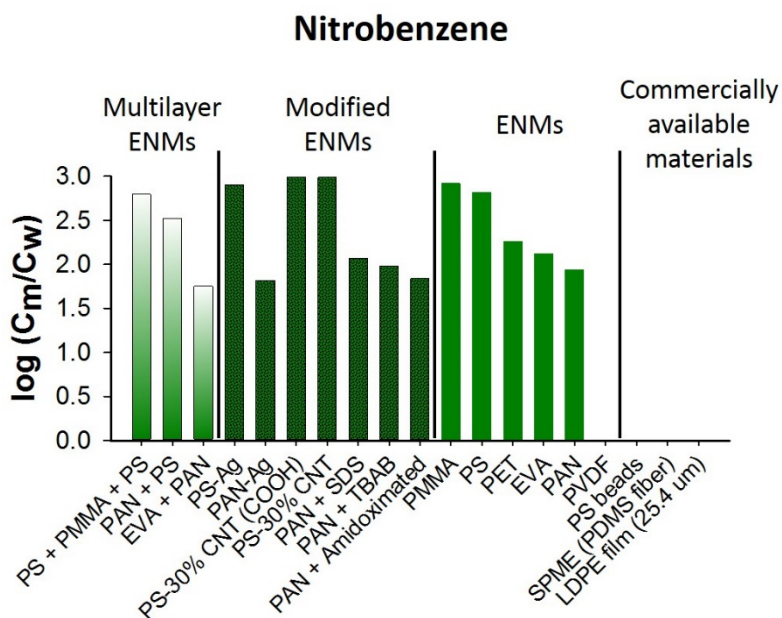


Figure 24. Summary of the ENM-water equilibrium partition coefficients for nitrobenzene obtained for all of the ENMs synthesized. Commercially available materials were also included, such as PS beads, PDMS fiber and LDPE film.

A similar comparison of partition coefficients for ENMs and conventional materials is shown in **Figure 25** for PCB47 and dioxin. Interestingly, ENM partition coefficients for PCB47 were roughly constant across all polymers we explored, and notably were also comparable to estimated partition coefficients for commercially available materials, such as a polyoxymethylene (POM) film, SPME (PDMS glass fiber) and LDPE film (low-density polyethylene) (1). We note that the partition coefficients for commercially available passive sampling materials were estimated from previously established laboratory correlations between measured partition coefficients and K_{ow} [i.e., $\log K_d = a \cdot \log K_{ow} + b$ (1, 61)]. For dioxin, we observed some variability in measured partition coefficients on ENMs, with PMMA-ENM yielding the highest value that is comparable to estimated partition coefficient values from LDPE film (61). As mentioned previously (see **Table 9**), the addition of oxidized and non-functionalized CNTs to PS resulted in a small reduction in the experimentally measured partition coefficient.

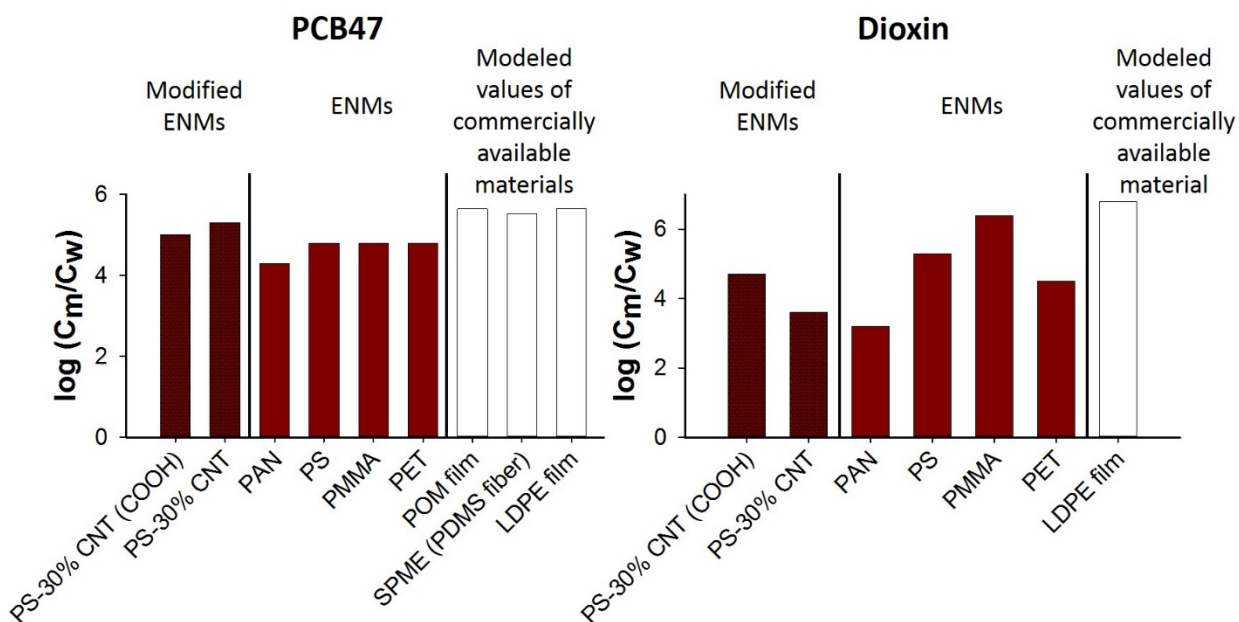


Figure 25. Summary of the ENM-water equilibrium partition coefficients for PCB47 (left panel) and dioxin (right panel) obtained for select ENMs, modified ENMs with CNTs. Also presented are estimated partition coefficients for commercially available materials, such as POM film, SPME (PDMS fiber) and LDPE film (1, 61).

Ultimately, given the superior performance of ENMs relative to commercial options for polar analytes, and their near identical performance with commercial options for hydrophobic targets, we contend that ENMs are an attractive option for next-generation passive sampling materials. Further, because we did not observe any inhibition via competitive uptake between hydrophilic and hydrophobic analytes herein, ENMs hold the promise of simultaneous, multi-target uptake for mixtures of diverse chemical pollutants.

Freely-Dissolved Pore Water Measurements

Spiked Model Soil Systems

A final set of “proof-of-concept” experiments with ENMs were conducted in more complex, heterogeneous (i.e., two-phase) systems containing contaminated water and soil. These systems were critical for validating performance for pore water measurement in more environmentally relevant systems, where competition with soil or soluble natural organic matter could diminish performance and complicate analysis of field deployed ENMs (56).

Results from these pore water measurement experiments with nitrobenzene are shown in **Figure 26**, which were conducted using a commercially available sandy loam with ~3% soil organic matter. The pore water concentration was calculated using the mass of the chemical accumulated in the ENM (m_i), the mass of the ENM used in the experiments (m_{ENM}) and the equilibrium partition coefficients measured from our aqueous-phase uptake experiments (K_{Di}) (**Table 6**), using the following equation:

$$C_{pwi} = m_i / (K_{Di} \times m_{ENM}) \quad \text{Equation 1}$$

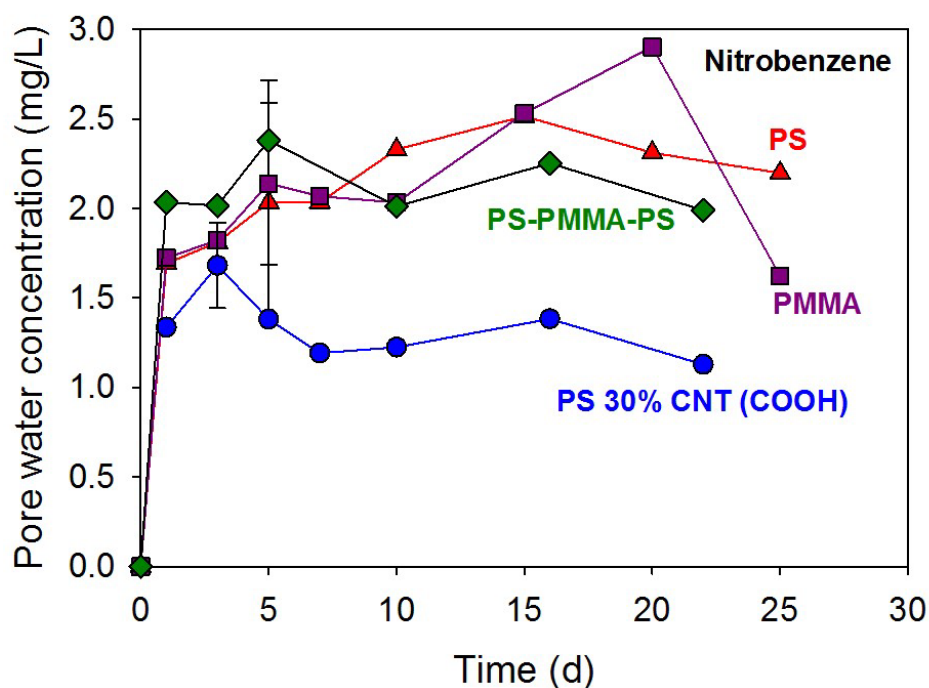


Figure 26. Laboratory pore water measurements of nitrobenzene from our model spiked soil using PS, PMMA, PS-CNT (functionalized) and PS-PMMA-PS ENMs. Lines are drawn as guide to the eye.

Four ENMs were tested, representing a suite of the most promising materials prioritized in earlier uptake studies. These included PS-ENM, PMMA-ENM, as well as PS amended with functionalized CNTs (i.e., with COOH surface sites) and a tri-layer ENM in a sandwich configuration with PS and PMMA (i.e., PS-PMMA-PS) (see schematic **Figure 7**).

All materials achieved rapid equilibrium with pore water nitrobenzene (< 1 day). Effectively, PS-ENM, PMMA-ENM and the tri-layer structure were equivalent in performance, with equilibrium pore water concentrations ranging between 1.7 and 2.8 mg/L for these samples. The relative performance of these materials is consistent with results from our simpler, homogeneous systems, where all three ENMs also exhibited near identical performance (see **Figure 23** and **Figure 24**). Notably, the measured pore water concentration with CNT-modified materials was noticeably less than with the other materials. We believe this may be due to more uptake of non-target organic matter facilitated by the CNTs, thereby inhibiting nitrobenzene uptake.

An important outcome of these studies was our realization that PS-ENM is relatively resistant to fouling in (sterilized) soil systems. Specifically, after 5 d of mixing with soil, PS-ENM was considerably easier to clean of debris and wash than other ENMs (**Figure 27**). After a gentle mechanical cleaning with a paper towel and a light rinse with a small volume of DI water [for which loss of nitrobenzene was measured to be rather small (< 5%)], the PS-ENM was nearly the same color as freshly synthesized materials. SEM images of the rinsed PS-ENM also revealed no residual particles (**Figure 27**). Similar behavior was not observed for PMMA-ENM, which remained covered in soil and organic particles (both observable to the naked eye and by SEM; images not shown) even after more extensive washing with DI water. We believe these complications affected the general reproducibility of our results with PMMA, where measured pore water concentrations varied more considerably over time than with other ENMs.

We emphasize that the much easier cleanup of PS after application in soil is a tremendous advantage for passive sampler development. This should increase performance in the field, as a result of slower fouling by organic matter. It should also increase the ease of sample processing after deployment, where cleaner ENMs will be easier to extract with less interference from non-target materials in the background matrix. In fact, our motivation for including a PS-PMMA-PS tri-layer material was to utilize this behavior of PS to protect PMMA from organic fouling during application, and we are tremendously encouraged by greater consistency in pore water nitrobenzene concentrations measured with this tri-layer ENM.

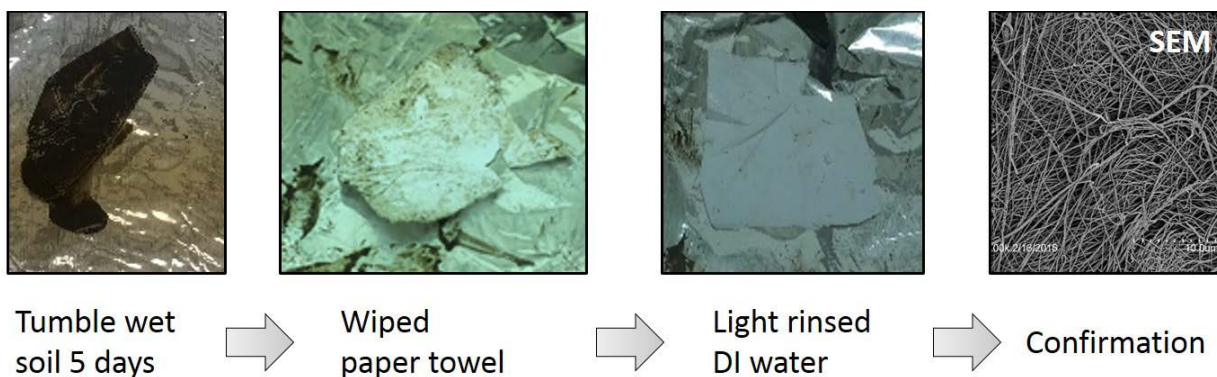


Figure 27. Photograph sequence of cleaning for PS-ENM after being exposed to model soils for 5 days.

For aniline, laboratory pore water measurements in model soil systems were most stable for tri-layer PS-PMMA-PS, with rapid equilibrium (< 5 day) and stable pore water concentrations of

~1.5 mg/L (**Figure 28**). Notably, reliable values for aniline pore water concentration were only obtained with this tri-layer ENM, which we attribute to (i) the favorable uptake of polar aniline by hydrophilic PMMA and (ii) the protection from organic matter fouling by PS layers sandwiched around the active, middle PMMA layer. For example, use of PMMA alone resulted in significant residual soil associated with the mat, and aniline associated with these soil particles interfered with attempts to measure pore water concentration. Accordingly, use of PMMA without protective PS layers produced highly variable and unreliable pore water aniline concentrations that reached values in excess of 5.0 mg/L. *The far superior performance of the tri-layer ENM illustrates their promise, enabling the use of high capacity hydrophilic passive sampling materials with fewer concerns over their interactions with non-target organic matter in complex natural systems.*

Although we are not certain why pore water measurements of aniline in our spiked soil experiments are not stable as nitrobenzene, these types of experiments and outcomes are very valuable for future passive sampler development.

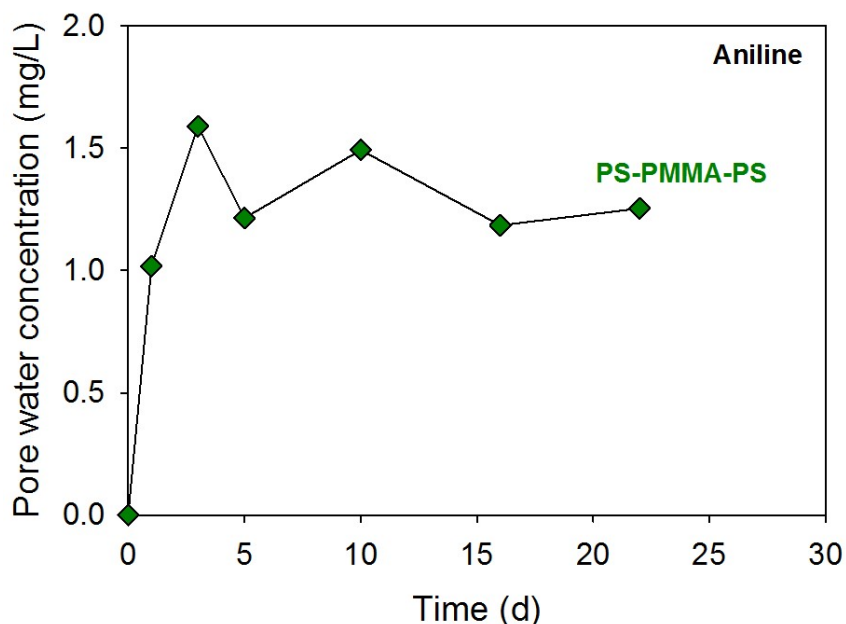


Figure 28. Laboratory pore water measurements of aniline from our model spiked soil using PS-PMMA-PS ENMs. Lines are drawn as guide to the eye.

Regarding PCBs in the spiked soil system, PS-ENM detected all six PCB congeners (PCB1, 11, 29, 47, 121 and 136). Utilizing Equation 1, calculated sediment pore water concentrations ranged from 20 ng/L to 1300 ng/L (PCB1 = 1300, PCB11 = 740, PCB29 = 120, PCB47 = 250, PCB121 = 70 and PCB136 = 20 ng/L). Although this experiment was performed for only 5 days, which may indicate that the sediment pore water concentration and the PS-ENM did not reach equilibrium, these pore water concentration values are in accordance with the amount spiked to the soil. No issues were observed regarding the cleaning of the ENM for PCBs.

Contaminated Sediment Systems

To further explore the applicability and performance of ENMs as passive sampling materials, we tested PS-ENM and PMMA-ENM in a “real-world” anthropogenic-contaminated sediment. Results from 50 days exposure to the sediments showed that only PCBs were measured by our ENMs. Aniline, nitrobenzene and dioxin were not detected, although they were not expected to be present at this contaminated site (IHSC), which has a legacy of PCB contamination. In fact, to the best of our knowledge, there are no reports of aniline, nitrobenzene or dioxin in the IHSC sediments (62).

The six PCB congeners (PCB1, 11, 29, 47, 121 and 136) were detected and measured using the mass accumulated in the ENM over time, the mass of the ENMs used in the experiments, and the partition coefficient previously measured in homogeneous (aqueous) systems (**Table 7**). Sediment pore water concentrations ranged from 0.1 to 20.0 pg/L for the individual congeners (**Figure 29**). Both ENMs performed similarly, where no significant difference was observed between measured sediment pore water concentrations. In general, less chlorinated congeners yielded higher concentrations, where the more hydrophobic congeners yielded lower concentration values. This trend is consistent with their hydrophobicity, as the more hydrophobic congeners are expected to more readily associate with the organic-rich sediment particles. Once again, PS-ENM was far easier to clean than PMMA-ENM, highlighting its potential value in complex and “dirty” environmental systems.

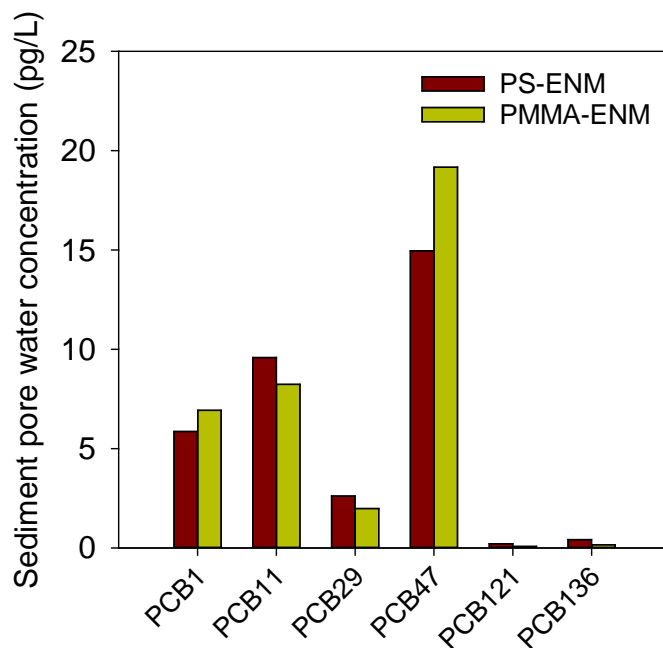


Figure 29. Sediment pore water concentration measurements in pg/L carried out using PS-ENM and PMMA-ENM. 30 grams of wet sediment from IHSC with ENMs were tumbled for 50 days.

We are greatly encouraged by these results, which validate our proof-of-concept research efforts. *Indeed, these results from complex sediment and soil systems demonstrate that our passive*

sampling materials are readily applicable to diverse chemical pollutant classes in “real world” systems. This includes hydrophobic legacy compounds such as PCBs present in contaminated sediments, where ENM application can be used to produce a very low detection limit (~pg/L).

Conclusions and Implications for Future Research

Key Results

Over the past year of SERDP support, we have executed an experimental plan that successfully achieved the objectives outlined in our original SEED proposal. Via this proof-of-concept investigation, we have demonstrated for the first time that electrospun nanofiber mats (ENMs) represent viable materials for use in passive sampling devices. More importantly, results generated herein reveal the immense promise of ENMs, thereby eliminating any risks associated with further research into their development, optimization and application as passive sampling devices for environmental monitoring at complex, extensively contaminated sites of relevance to DOD.

Our most notable results include:

- Reproducible synthesis of ENMs (see **Figure 10** and **Table 4**), thereby achieving our first metric for project success.
- Tunable synthesis of ENMs that allows physical and chemical properties of ENMs to be easily controlled for optimizing performance (see **Figure 11**)
- Several polymer ENMs represent viable sorbent materials for simultaneous uptake of both hydrophilic and hydrophobic targets of relevance to contaminated DOD sites.
- No adverse or inhibitory effect on ENM performance during their application to complex and diverse chemical pollutant mixtures.
- Optimal ENMs that exhibit uptake kinetics and partition coefficients often exceeding (by wide margins; e.g., 3-log units for aniline uptake) current commercially available passive sampling materials (**Figure 23** and **Figure 24**), thereby achieving our second metric for project success.
- Consistent and reliable performance results across a range of environmentally relevant conditions including homogeneous (e.g., water column) and heterogeneous (e.g., sediment and soil) systems, thereby achieving our third metric for project success.
- One pot synthesis of chemically modified ENMs or ENM composites with unique surface chemical (e.g., surface charge via surfactants to promote favorable electrostatics; biocidal activity of integrated Ag nanoparticles) or physical properties (e.g., benefits of strength from embedded CNTs) to further enhance performance, handling and application.
- Multilayer ENMs that can be used to generate structures with additive, even synergistic, performance properties, particularly for cases where it may be advantageous to fabricate passive samplers with multiple sorbent layers each specifically designed to target a different pollutant class.

Tangible outcomes and products

Beyond these findings, there are also several tangible outcomes and products of this SEED investigation that will be of immediate value to the community of researchers and practitioners focused on passive sampling technologies. Through dissemination of our results, including a

manuscript draft in preparation and presentations at professional meetings, these outcomes and products will be immediately available and ready for use by SERDP and DOD regardless of any additional commitment for future research support or follow-up investigations. Specific outcomes and products include:

- Recipes for the synthesis of a suite of polymer ENMs with tunable physical and chemical properties that can outperform currently available forms of passive sampling materials and are therefore ready for future scale-up and prototyping for industrial application.
- Analytical methods, including laboratory protocols, for the application and extraction of polymer ENMs in complex media, including sediments and pollutant mixtures.
- Best practices for further optimizing the performance and practical application of ENMs to increase ease of use in complex media (e.g., demonstration of biocidal materials for antifouling) and pollutant mixtures (e.g., multilayer structures for simultaneous targeting of chemically diverse pollutant classes).

Overarching implications of SEED project results and outcomes

Finally, there are broad implications stemming from the results and outcomes this SEED project, including:

- Discovery of innovative nanoenabled materials with the potential to expand the use and increase the reliability of passive sampling devices.
- Improved site characterization via the small material footprint of ENMs that should allow better spatial resolution of data, while fast rates of uptake will allow for better temporal resolution of data.
- The potential for rapid scale up and transition of this technology to the commercial marketplace because electrospinning is already an industrially viable fabrication process for non-woven polymers (27).

Opportunities for future research

While the results to date have been incredibly promising, more work is needed to fully realize the promise of ENMs as next-generation passive sampling materials. This proof-of-concept work, while successful, only provides the foundation for future research to further improve ENM fabrication and application. Consequently, the PI team would like to request the opportunity to draft a proposal for follow-up support from SERDP, funds from which would be used to build upon current ENM formulations and promote their more rapid translation to the commercial marketplace (27).

Specific objectives for such a proposal, along with a brief description of associated tasks, are as follows:

- **Future Objective 1: Increase capacity and rate of uptake for ENMs toward a broader suite of DOD relevant analytes.** Rationale and Needs Addressed: The SEED grant has demonstrated the promise of polymer ENMs, as well as strategic modifications (e.g., surfactants) to improve their uptake rates and capacity. However, our proof-of-concept SEED project was limited in scope (due to its short duration), only focusing on a small suite of model analytes. Moreover, only a relatively small number of the promising fabrication approaches proposed to improve ENM performance were explicitly

demonstrated. General Approach: We will expand the analyte suite to include a broader range of DOD relevant targets including munitions components [TNT and RDX (8)], their polar metabolites, and emerging insensitive munitions (IMX). While additional work with hydrophobic PCBs will also be conducted (expanding upon work conducted herein), the potential for ENMs to function as passive sampling materials for other high priority, emerging and recalcitrant pollutants (e.g., 1,4 dioxane and PFCs) will also be examined. For ENMs, additives (e.g., CNTs and ionic surfactants) will be integrated into more materials than the few demonstrated herein. Also, experiments will utilize stagnant soil and water systems so as to truly measure uptake in a passive system (whereas experiments conducted herein were mixed actively due to the short duration of the SEED project). Finally, as in ter Laak *et al.* (56), uptake and elimination rates will be measured to help optimize the design of ENMs for application either in the equilibrium- or kinetic-controlled regimes.

- **Future Objective 2: Develop mechanistic insights and predictive linear free energy relationships to promote optimal ENM application.** Rationale and Needs Addressed: A major shortcoming of current commercial polar passive samplers (e.g., POCIS) is a general lack of understanding as to the forces responsible for pollutant uptake (13, 14). Ultimately, this lack of fundamental, mechanistic knowledge limits passive sampler application because of uncertainty over the pollutant targets best suited for analysis, lack of understating of the uptake mode of the passive sampler during field deployment (integrated vs. equilibrium) and potential interference of unwanted materials into the sampler (e.g. natural organic matter). General Approach: With partition coefficients from a broader suite of chemically diverse analytes and polymer ENMs, we intend to develop poly-parameter linear free energy relationships (ppLFEs) that will not only provide mechanistic insights into pollutant uptake but also allow prediction of other compound classes that could be effectively targeted by chemically modified ENMs. In addition to the analytes identified in the previous objective, uptake experiments will also be conducted with a range of well-characterized model compounds [e.g., structurally related substituted benzenes and phenols (12)], thereby facilitating ppLFE construction. Further, we also intend to examine a range of analytes commonly targeted using POCIS (8), thereby allowing direct comparisons between ENM and the current “gold standard” for polar organic uptake.
- **Future Objective 3: Enhance selectivity of ENMs toward highest priority DOD targets.** Rationale and Needs Addressed: In the most complex of contaminated media, highly selective uptake of high priority pollutants can be advantageous, thereby simplifying analysis of bound mass after passive sampler solvent extraction. General Approach: Molecularly imprinted polymers (or MIPs) represent an innovative approach for the highly specific binding of target analytes. MIPs are fabricated by including the target analyte into polymers during their synthesis, after which the materials are thoroughly washed to remove the target analyte. This leaves behind a cavity highly specific for analyte binding (63), evocative of the “lock-and-key” receptor binding interaction for bioactive chemicals. Here, we will synthesize electrospun MIPs for high priority, polar analytes (e.g., TNT and RDX), and test their performance relative to non-imprinted ENMs. Recently, advances have been made to allow for the production of

MIPs via electrospinning (64), but this approach has not yet been utilized for environmental monitoring and passive sampling development.

- **Future Objective 4: Demonstrate the increased functionality of chemically tailored ENMs in complex media.** Rationale and Needs Addressed: While work in this SEED grant demonstrated the promise of chemically modified ENMs, the range of benefits afforded by certain materials (e.g., Ag-modified ENMs for slowing biofouling or multilayer ENMs to limit organic matter interference) have not been rigorously quantified. General Approach: This work will focus on the most promising of modified ENMs, explicitly testing performance aspects indirectly related to pollutant uptake. For Ag- and TBAB-modified materials, tests will be conducted to observe their rate of biofouling in sediment systems relative to unmodified materials. For PS-containing multilayer options, their ability to resist interference from soil organic matter will also be quantitatively evaluated. A key variable in these trials will be the duration of testing for each modified-ENM, where the viable lifetime of materials will be determined (i.e., performance over longer time scales than typically investigated herein, from several weeks to months).
- **Future Objective 5: Fabricate and field test an ENM-enabled, multi-target passive sampling device.** Rationale and Needs Addressed: All work to date has been conducted in model systems at the laboratory scale. To promote technology translation, prototyping and scale up of an ENM-enabled passive sampling device is needed, as are field data demonstrating the reliability of this approach and potential advantages it holds over current commercially available passive sampling devices. General Approach: A passive sampling device will be fabricated using optimal ENMs. The best ENM for scale up and prototype development will be based upon our laboratory results from the SEED project and the aforementioned follow-up studies, as well as life cycle analysis (LCA) that will be conducted to guide the sustainable design of ENMs whose manufacturing results in the least environmental impact (65-67). For field testing, we intend to partner with an existing SERDP project and contaminated DOD site that will allow for the deployment of the ENM-enabled passive sampler. We will also conduct a side-by-side performance comparison with a commercially available passive sampling device already in operation at the site to help establish the benefits of ENM-based passive sampling devices relative to current commercially available options.

We would anticipate a three-year follow-up study, with an estimated budget of approximately \$750,000 to complete the stated tasks and achieve these future objectives.

Literature Cited

1. Ghosh, U.; Kane Driscoll, S.; Burgess, R. M.; Jonker, M. T. O.; Reible, D.; Gobas, F.; Choi, Y.; Apitz, S. E.; Maruya, K. A.; Gala, W. R.; Mortimer, M.; Beegan, C., Passive sampling methods for contaminated sediments: Practical guidance for selection, calibration, and implementation. *Integr Environ Assess Manag* **2014**, *10*, (2), 210-223.
2. Greenwood, R.; Mills, G.; Vrana, B., *Comprehensive Analytical Chemistry: Passive sampling techniques in environmental monitoring*. Elsevier Publishing Company: 2007.
3. Jonker, M. T. O.; Koelmans, A. A., Polyoxymethylene solid phase extraction as a partitioning method for hydrophobic organic chemicals in sediment and soot. *Environ Sci Technol* **2001**, *35*, (18), 3742-3748.
4. Martinez, A.; O'Sullivan, C.; Reible, D.; Hornbuckle, K. C., Sediment pore water distribution coefficients of PCB congeners in enriched black carbon sediment. *Environ Pollut* **2013**, *182*, (0), 357-363. PMID: 23974165; PMC3833079.
5. Mayer, P.; Wania, F.; Wong, C. S., Advancing passive sampling of contaminants in environmental science. *Env Sci Process Impact* **2014**, *16*, (3), 366-368.
6. Alvarez, D. A., Development of semipermeable membrane devices (SPMDs) and polar organic chemical integrative samplers (POCIS) for environmental monitoring. *Environ Toxicol Chem* **2013**, *32*, (10), 2179-2181.
7. Alvarez, D. A.; Petty, J. D.; Huckins, J. N.; Jones-Lepp, T. L.; Getting, D. T.; Goddard, J. P.; Manahan, S. E., Development of a passive, in situ, integrative sampler for hydrophilic organic contaminants in aquatic environments. *Environ Toxicol Chem* **2004**, *23*, (7), 1640-1648.
8. Belden, J. B.; Lotufo, G. R.; Biedenbach, J. M.; Sieve, K. K.; Rosen, G., Application of POCIS for exposure assessment of munitions constituents during constant and fluctuating exposure. *Environ Toxicol Chem* **2015**, *34*, (5), 959-967.
9. George, T. S.; Vlahos, P.; Hamer, T.; Helm, P.; Wilford, B., A rapidly equilibrating, thin film, passive water sampler for organic contaminants; characterization and field testing. *Environ Pollut* **2011**, *159*, (2), 481-486.
10. Metcalfe, C.; Hoque, M. E.; Sultana, T.; Murray, C.; Helm, P.; Kleywegt, S., Monitoring for contaminants of emerging concern in drinking water using POCIS passive samplers. *Env Sci Process Impact* **2014**, *16*, (3), 473-481.
11. Mills, G. A.; Gravell, A.; Vrana, B.; Harman, C.; Budzinski, H.; Mazzella, N.; Ocelka, T., Measurement of environmental pollutants using passive sampling devices - an updated commentary on the current state of the art. *Env Sci Process Impact* **2014**, *16*, (3), 369-373.
12. Bauerlein, P. S.; Mansell, J. E.; ter Laak, T. L.; de Voogt, P., Sorption Behavior of Charged and Neutral Polar Organic Compounds on Solid Phase Extraction Materials: Which Functional Group Governs Sorption? *Environ Sci Technol* **2012**, *46*, (2), 954-961.
13. Harman, C.; Allan, I. J.; Bauerlein, P. S., The Challenge of Exposure Correction for Polar Passive Samplers-The PRC and the POCIS. *Environ Sci Technol* **2011**, *45*, (21), 9120-9121.
14. Harman, C.; Allan, I. J.; Vermeirssen, E. L. M., Calibration and use of the polar organic chemical integrative sampler-a critical review. *Environ Toxicol Chem* **2012**, *31*, (12), 2724-2738.

15. Nataraj, S. K.; Yang, K. S.; Aminabhavi, T. M., Polyacrylonitrile-based nanofibers A state-of-the-art review. *Prog Polym Sci* **2012**, *37*, (3), 487-513.
16. Sawada, K.; Sakai, S.; Taya, M., Enhanced productivity of electrospun polyvinyl alcohol nanofibrous mats using aqueous N,N-dimethylformamide solution and their application to lipase-immobilizing membrane-shaped catalysts. *J Biosci Bioeng* **2012**, *114*, (2), 204-208.
17. Huang, Z. M.; Zhang, Y. Z.; Kotaki, M.; Ramakrishna, S., A review on polymer nanofibers by electrospinning and their applications in nanocomposites. *Compos Sci Technol* **2003**, *63*, (15), 2223-2253.
18. Ma, Z. W.; Kotaki, M.; Yong, T.; He, W.; Ramakrishna, S., Surface engineering of electrospun polyethylene terephthalate (PET) nanofibers towards development of a new material for blood vessel engineering. *Biomaterials* **2005**, *26*, (15), 2527-2536.
19. Lu, P.; Ding, B., Applications of Electrospun Fibers. *Recent Pat Nanotechnol* **2008**, *2*, (3), 169-182.
20. Zhou, F.-L.; Gong, R.-H., Manufacturing technologies of polymeric nanofibres and nanofibre yarns. *Polym Int* **2008**, *57*, (6), 837-845.
21. Zeng, S.; Baillargeat, D.; Ho, H.-P.; Yong, K.-T., Nanomaterials enhanced surface plasmon resonance for biological and chemical sensing applications. *Chem Soc Rev* **2014**, *43*, (10), 3426-3452.
22. Jadhav, A. H.; Mai, X. T.; Ofori, F. A.; Kim, H., Preparation, characterization, and kinetic study of end opened carbon nanotubes incorporated polyacrylonitrile electrospun nanofibers for the adsorption of pyrene from aqueous solution. *Chem Eng J* **2015**, *259*, 348-356.
23. Liang, D.; Hsiao, B. S.; Chu, B., Functional electrospun nanofibrous scaffolds for biomedical applications. *Adv Drug Deliver Rev* **2007**, *59*, (14), 1392-1412.
24. North Carolina State University The Nonwovens Institute.
<https://thenonwovensinstitute.com>
25. Barnes, C. P.; Sell, S. A.; Boland, E. D.; Simpson, D. G.; Bowlin, G. L., Nanofiber technology: Designing the next generation of tissue engineering scaffolds. *Adv Drug Deliver Rev* **2007**, *59*, (14), 1413-1433.
26. Corey, J. M.; Lin, D. Y.; Mycek, K. B.; Chen, Q.; Samuel, S.; Feldman, E. L.; Martin, D. C., Aligned electrospun nanofibers specify the direction of dorsal root ganglia neurite growth. *J Biomed Mater Res Part A* **2007**, *83A*, (3), 636-645.
27. Persano, L.; Camposeo, A.; Tekmen, C.; Pisignano, D., Industrial Upscaling of Electrospinning and Applications of Polymer Nanofibers: A Review. *Macromol Mater Eng* **2013**, *298*, (5), 504-520.
28. Uyar, T.; Besenbacher, F., Electrospinning of uniform polystyrene fibers: The effect of solvent conductivity. *Polymer* **2008**, *49*, (24), 5336-5343.
29. Choi, S. S.; Lee, Y. S.; Joo, C. W.; Lee, S. G.; Park, J. K.; Han, K. S., Electrospun PVDF nanofiber web as polymer electrolyte or separator. *Electrochim Acta* **2004**, *50*, (2-3), 339-343.
30. Ghochaghi, N.; Taiwo, A.; Winkel, M.; Dodd, B.; Mossi, K.; Tepper, G., Electrospun Polystyrene Coatings with Tunable Wettability. *J Appl Polym Sci* **2015**, *132*, (10).
31. Jannesari, M.; Varshosaz, J.; Morshed, M.; Zamani, M., Composite poly(vinyl alcohol)/poly(vinyl acetate) electrospun nanofibrous mats as a novel wound dressing matrix for controlled release of drugs. *Int J Nanomedicine* **2011**, *6*, 11.

32. Jarusuwannapoom, T.; Hongrojjanawiwat, W.; Jitjaicham, S.; Wannatong, L.; Nithitanakul, M.; Pattamaprom, C.; Koombhongse, P.; Rangkupan, R.; Supaphol, P., Effect of solvents on electro-spinnability of polystyrene solutions and morphological appearance of resulting electrospun polystyrene fibers. *Eur Polym J* **2005**, *41*, (3), 409-421.
33. Kim, J. R.; Choi, S. W.; Jo, S. M.; Lee, W. S.; Kim, B. C., Electrospun PVdF-based fibrous polymer electrolytes for lithium ion polymer batteries. *Electrochim Acta* **2004**, *50*, (1), 69-75.
34. Lee, J. S.; Choi, K. H.; Do Ghim, H.; Kim, S. S.; Chun, D. H.; Kim, H. Y.; Lyoo, W. S., Role of molecular weight of atactic poly(vinyl alcohol) (PVA) in the structure and properties of PVA nanofabric prepared by electrospinning. *J Appl Polym Sci* **2004**, *93*, (4), 1638-1646.
35. Liu, Y.; Li, C.; Chen, S.; Wachtel, E.; Koga, T.; Sokolov, J. C.; Rafailovich, M. H., Electrospinning of Poly(ethylene-co-vinyl acetate)/Clay Nanocomposite Fibers. *J Polym Sci Pol Phys* **2009**, *47*, (24), 2501-2508.
36. Piperno, S.; Lozzi, L.; Rastelli, R.; Passacantando, M.; Santucci, S., PMMA nanofibers production by electrospinning. *Appl Surf Sci* **2006**, *252*, (15), 5583-5586.
37. Veleirinho, B.; Lopes-da-Silva, J. A., Application of electrospun poly(ethylene terephthalate) nanofiber mat to apple juice clarification. *Process Biochem* **2009**, *44*, (3), 353-356.
38. Wang, T.; Kumar, S., Electrospinning of polyacrylonitrile nanofibers. *J Appl Polym Sci* **2006**, *102*, (2), 1023-1029.
39. Xu, C.; Xu, F.; Wang, B.; Lu, T., Electrospinning of Poly(ethylene-co-vinyl alcohol) Nanofibres Encapsulated with Ag Nanoparticles for Skin Wound Healing. *J Nanomater* **2011**.
40. Saeed, K.; Haider, S.; Oh, T.-J.; Park, S.-Y., Preparation of amidoxime-modified polyacrylonitrile (PAN-oxime) nanofibers and their applications to metal ions adsorption. *J Membrane Sci* **2008**, *322*, (2), 400-405.
41. Peter, K. T.; Vargo, J. D.; Rupasinghe, T. P.; De Jesus, A.; Tivanski, A. V.; Sander, E. A.; Myung, N. V.; Cwiertny, D. M., Synthesis, Optimization, and Performance Demonstration of Electrospun Carbon Nanofiber-Carbon Nanotube Composite Sorbents for Point-of-Use Water Treatment. *Acs Appl Mater Interfaces* **2016**, *8*, (18), 11431-11440.
42. US Government Accountability Office (GAO) *Hazardous Water Cleanup. Numbers of Contaminated Federal Sites, Estimated Costs, and EPA's Oversight Role. GAO-15-830T*; 2015.
43. Hawthorne, S. B.; Grabanski, C. B.; Miller, D. J.; Arp, H. P. H., Improving Predictability of Sediment-Porewater Partitioning Models using Trends Observed with PCB-Contaminated Field Sediments. *Environ Sci Technol* **2011**, *45*, (17), 7365-7371.
44. Lambert, M. K.; Friedman, C.; Luey, P.; Lohmann, R., Role of Black Carbon in the Sorption of Polychlorinated Dibenzo-p-dioxins and Dibenzofurans at the Diamond Alkali Superfund Site, Newark Bay, New Jersey. *Environ Sci Technol* **2011**, *45*, (10), 4331-4338.
45. Martinez, A.; Norström, K.; Wang, K.; Hornbuckle, K. C., Polychlorinated biphenyls in the surficial sediment of Indiana Harbor and Ship Canal, Lake Michigan. *Environ Int* **2010**, *36*, (8), 849-854.

46. Villacanas, F.; Pereira, M. F. R.; Orfao, J. J. M.; Figueiredo, J. L., Adsorption of simple aromatic compounds on activated carbons. *J. Colloid Interface Sci.* **2006**, *293*, (1), 128-136.
47. Vaes, W. H. J.; Ramos, E. U.; Verhaar, H. J. M.; Seinen, W.; Hermens, J. L. M., Measurement of the free concentration using solid-phase microextraction: Binding to protein. *Anal Chem* **1996**, *68*, (24), 4463-4467.
48. van Noort, P. C. M.; Haftka, J. J. H.; Parsons, J. R., Updated Abraham Solvation Parameters for Polychlorinated Biphenyls. *Environ Sci Technol* **2010**, *44*, (18), 7037-7042.
49. Hawker, D. W.; Connell, D. W., Octanol-water partition coefficients of polychlorinated biphenyl congeners. *Environ Sci Technol* **1988**, *22*, (4), 382-387.
50. Shiu, W. Y.; Doucette, W.; Gobas, F.; Andren, A.; Mackay, D., Physical-chemical properties of chlorinated dibenzo-para-dioxins. *Environ Sci Technol* **1988**, *22*, (6), 651-658.
51. Åberg, A.; MacLeod, M.; Wiberg, K., Physical-Chemical Property Data for Dibenzo-p-dioxin (DD), Dibenzofuran (DF), and Chlorinated DD/Fs: A Critical Review and Recommended Values. *J Phys Chem Ref Data* **2008**, *37*, (4), 1997-2008.
52. Qu, S.; Kolodziej, E. P.; Cwiertny, D. M., Sorption and Mineral-Promoted Transformation of Synthetic Hormone Growth Promoters in Soil Systems. *J Agr Food Chem* **2014**, *62*, (51), 12277-12286.
53. Martinez, A.; Hornbuckle, K. C., Record of PCB congeners, sorbents and potential toxicity in core samples in Indiana Harbor and Ship Canal. *Chemosphere* **2011**, *85*, (3), 542-547.
54. Riggin, R. M.; Lucas, S. V.; Cole, T. F.; Birts, M. A. *Analytical procedures for aniline and selected derivatives in wastewater and sludge*; USEPA: Cincinnati, OH, 1984.
55. Wolfe, N. L.; Carreira, L. H.; Delgado, M. C., Method and composition for remediating environmental contaminants. WO1994023857 A1. In Google Patents: 1994.
56. ter Laak, T. L.; Busser, F. J. M.; Hermens, J. L. M., Poly(dimethylsiloxane) as passive sampler material for hydrophobic chemicals: Effect of chemical properties and sampler characteristics on partitioning and equilibration times. *Anal Chem* **2008**, *80*, (10), 3859-3866.
57. Vaes, W. H. J.; Hamwijk, C.; Ramos, E. U.; Verhaar, H. J. M.; Hermens, J. L. M., Partitioning of organic chemicals to polyacrylate-coated solid phase microextraction fibers: Kinetic behavior and quantitative structure-property relationships. *Anal Chem* **1996**, *68*, (24), 4458-4462.
58. Horzum, N.; Shahwan, T.; Parlak, O.; Demir, M. M., Synthesis of amidoximated polyacrylonitrile fibers and its application for sorption of aqueous uranyl ions under continuous flow. *Chem Eng J* **2012**, *213*, 41-49.
59. Zodrow, K.; Brunet, L.; Mahendra, S.; Li, D.; Zhang, A.; Li, Q.; Alvarez, P. J. J., Polysulfone ultrafiltration membranes impregnated with silver nanoparticles show improved biofouling resistance and virus removal. *Water Res* **2009**, *43*, (3), 715-723.
60. Lundin, J. G.; Coneski, P. N.; Fulmer, P. A.; Wynne, J. H., Relationship between surface concentration of amphiphilic quaternary ammonium biocides in electrospun polymer fibers and biocidal activity. *React Funct Polym* **2014**, *77*, 39-46.

61. Adams, R. G.; Lohmann, R.; Fernandez, L. A.; Macfarlane, J. K.; Gschwend, P. M., Polyethylene devices: Passive samplers for measuring dissolved hydrophobic organic compounds in aquatic environments. *Environ Sci Technol* **2007**, *41*, (4), 1317-1323.
62. US Fish and Wildlife Service *An Assessment of Sediment Injury in the Grand Calumet River, Indiana Harbor Canal, Indiana Harbor, and the Nearshore Areas of Lake Michigan*; 2000.
63. Zhang, Y.; Wei, Q.; Zhang, Q.; Li, J.; Yang, J.; Zhao, C., Molecularly Imprinted Electrospinning Polyethersulfone Nano-Scale Fibers for the Binding and Recognition of Bisphenol A. *Separ Sci Technol* **2011**, *46*, (10), 1615-1620.
64. Zaidi, S. A., Recent developments in molecularly imprinted polymer nanofibers and their applications. *Anal Methods* **2015**, *7*, (18), 7406-7415.
65. Hischer, R.; Walser, T., Life cycle assessment of engineered nanomaterials: State of the art and strategies to overcome existing gaps. *Sci Total Environ* **2012**, *425*, 271-282.
66. Meyer, D. E.; Curran, M. A.; Gonzalez, M. A., An Examination of Existing Data for the Industrial Manufacture and Use of Nanocomponents and Their Role in the Life Cycle Impact of Nanoproducts. *Environ Sci Technol* **2009**, *43*, (5), 1256-1263.
67. Pourzahedi, L.; Eckelman, M. J., Comparative life cycle assessment of silver nanoparticle synthesis routes. *Environ Sci Nano* **2015**, *2*, (4), 361-369.